LEVEL II

12

134400-11-F

Final Report

COASTAL REMOTE SENSING INVESTIGATIONS

VOLUME 2: BEACH ENVIRONMENT

ERIC S. KASISCHKE
Applications Division

DECEMBER 1980

AD A095692

Office of Naval Research
Geography Programs
Arlington, VA 22217
Contract No. N00014-78-C-0458

DTIC
ELECTE
MAR 2 1981
D

DISTRIBUTION STATEMENT A
Approved for public release;
Distribution Unlimited

ENVIRONMENTAL
RESEARCH INSTITUTE OF MICHIGAN
BOX 8618 • ANN ARBOR • MICHIGAN 48107

DTIC FILE COPY

X

81 2 27 092

(14) ERIM-134400-11-F-VOL-2

Unclassified

SECURITY CLASSIFICATION OF THIS PAGE (*When Data Entered*)

REPORT DOCUMENTATION PAGE		READ INSTRUCTIONS BEFORE COMPLETING FORM
1 REPORT NUMBER 134400-11-F	2 GOVT ACCESSION NO AD-A095692	3 RECIPIENT'S CATALOG NUMBER (9)
4 TITLE (*and Subtitle*) Final Technical Report (6) Coastal REMOTE SENSING INVESTIGATIONS, VOLUME 2, BEACH ENVIRONMENT		5 TYPE OF REPORT & PERIOD COVERED Final Technical Report
		6 PERFORMING ORG REPORT NUMBER 134400-11-F
7 AUTHOR(*s*) Eric S. Kasischke		8 CONTRACT OR GRANT NUMBER (*s*) (15) N00014-78-C-0458
9 PERFORMING ORGANIZATION NAME AND ADDRESS Environmental Research Institute of Michigan Applications Division, P.O. Box 8618 Ann Arbor, MI 48107		10 PROGRAM ELEMENT PROJECT TASK AREA & WORK UNIT NUMBERS (12) 96
11 CONTROLLING OFFICE NAME AND ADDRESS Geography Programs Office of Naval Research Arlington, VA 22217		(11) 12 REPORT DATE December 1980 13 NUMBER OF PAGES vii +
14 MONITORING AGENCY NAME AND ADDRESS (*if different from Controlling Office*)		15 SECURITY CLASS (*of this report*) Unclassified 15a DECLASSIFICATION/DOWNGRADING SCHEDULE

16 DISTRIBUTION STATEMENT (*of this Report*)

Distribution of this document is unlimited.

17 DISTRIBUTION STATEMENT (*of the abstract entered in Block 20, if different from Report*)

18 SUPPLEMENTARY NOTES

19 KEY WORDS (*Continue on reverse side if necessary and identify by block number*)

Beach Environment	Soil Moisture
Remote Sensing	Soil Mineralogy
Grain Size	Multispectral Scanner

20 ABSTRACT (*Continue on reverse side if necessary and identify by block number*)

An algorithm was developed which first classifies beach sands into one of five mineralogical classifications, then estimates grain size and soil moisture using equations based on actual and AQUASAND data. This algorithm was evaluated using "unknown" beach sand samples. The algorithm correctly identified the beach mineralogy in three out of the six cases, and the soil moisture estimates were in good agreement with the correctly predicted grain size. The algorithm was modified to classify airborne multispectral scanner data from (con't)

DD FORM 1 JAN 73 1473 EDITION OF 1 NOV 65 IS OBSOLETE

Unclassified

SECURITY CLASSIFICATION OF THIS PAGE (*When Data Entered*)

20. Abstract (continued)

two test sites (Lake Michigan and Panama City, Florida).

This report also contains sections on the use of satellite data as inputs into the MOGS algorithm and the development of similar algorithms for soils other than sand.

FORWARD

The work reported herein summarizes the final research activity in the Beach Environment Task of a program at ERIM entitled "Coastal Remote Sensing Investigations." The work has been performed under the guidance of Mr. Hans Dolezalek of the Office of Naval Research, Code 460.

This study was carried out in the Applications Division of the Environmental Research Institute of Michigan (ERIM). The principal investigator for the program was Dr. David R. Lyzenga while Mr. Eric S. Kasischke served as task leader for the project. Mr. Robert A. Shuchman supplied technical expertise for running the MOGS algorithm. Dr. Gwynn Suits contribution Section 6 dealing with the extension of the MOGS algorithm to silts and clays.

Accession For	
NTIS GRA&I	☒
DTIC TAB	☐
Unannounced	☐
Justification	
By	
Distribution/	
Availability Codes	
Dist	Avail and/or Special
A	

DTIC ELECTE MAR 2 1981 S D

D

TABLE OF CONTENTS

LIST OF FIGURES

LIST OF TABLES

1

INTRODUCTION

This report summarizes the final research activity in the Beach Environment task of a multi-year study at ERIM concerned with the problem of Coastal Remote Sensing. The purpose of the Beach Environment task was to study ways in which beach environmental parameters (soil particle size, moisture content, and mineralogical composition) could be remotely sensed. The remotely sensed beach parameters are then used as inputs in a trafficability/mobility model.

Included in this report is a summary of previous work accomplished under this program, as well as specifically reporting on final year activities. Scientific findings from this ONR supported study have been published in the open literature. The appendix to this report includes these reprints as background information.

In the final year of this effort, several analyses were performed. A more accurate and environmentally applicable mineralogy, moisture and grain size algorithm (MOGS) was developed using actual sand samples and inputs from the AQUASAND model. The MOGS algorithm first classifies the sand sample into one of five basic beach classifications. These classifications, based on mineralogical breakdowns, were performed via a minimum vector length technique. Next, the MOGS algorithm estimates the moisture and grain size using equations based on actual and AQUASAND data.

The MOGS algorithm was evaluated using "unknown" beach sand samples. The MOGS algorithm correctly identified the beach mineralogy in 3 out of 6 cases. The percent moisture estimates predicted by the algorithm were in good agreement with the actual moistures. There seems to be some doubt as to whether the MOGS algorithms can be used to accurately predict grain size. This failure is not serious from a beach trafficability standpoint, however, because recent studies have

shown that beach trafficability models are rather insensitive to grain size, when all other factors are considered (Thomson, et al., 1980).

The MOGS algorithm was then modified so that it could be used to classify data collected by the ERIM airborne multispectral scanner. Data from two sites were processed. One site was on the shores of Lake Michigan, near Muskegon, Michigan, while the other site was at Panama City, Florida.

The final sections of this report discuss the use of satellite data as inputs into the algorithms and the development of a MOGS type algorithm for soils other than sand.

2

BACKGROUND

The ability to remotely estimate composition of surface terrestrial materials has been demonstrated by many workers, and these results may have direct transfer value to beaches, where the composition is similar to that studied by geologists. The most prominent reports in this area have been by Vincent (1972, 1973), Vincent and Thomson (1972), and Vincent et al. (1972). These authors have explained the physical and optical properties of various rock and soil types as well as demonstrated the capabilities of a thermal infrared scanner in accurately classifying silica-containing soil and rock outcroppings and areas with surface iron stain. Discrimination is generally based on either atomic or ionic absorption in the shorter wavelengths (0.35 to 2.5 μm) and by lattice absorption at longer wavelengths (8 to 14 μm reststrahlen bands in silicate and carbonate minerals). These effect the spectral reflectance or emittance of materials.

Reststrahlen spectral emissivity variations with surface moisture have been studied by Watson (1970). He determined that as a thickness of water increased from 0 to 30 μm on a polished quartz slab, emittance increased at the principal quartz reststrahlen wavelengths of 8.5, 9.0, and 12.5 μm. This may be an important way to detect sample moisture content, and the effect will almost certainly influence compositional maps made of wet areas using the techniques reported by Vincent (1972, 1973).

Another qualitative observation is that the size of silicate mineral grains affects the reststrahlen emissivity features. Hovis and Callahan (1966) have demonstrated qualitatively that when the grain size of a sample is reduced from a solid sample to particles with diameters of 1-2 mm, 0.105-0.250 mm, and less than 0.038 mm, the measured reflectance progressively increases. Hunt and Vincent (1968)

have attempted to explain this phenomena in terms of a specular surface reflectance component (R_s) and a reflectance component which is due to radiation that has been transmitted through part or parts of the sample before re-emerging (R_v). The total sample reflectance is the sum of R_s and R_v. Further, the ratio R_s/R_v depends on grain size, because R_s and R_v depend differently on the absorption coefficient, a. Thus, the reflectance or emittance of the sample will depend on grain size.

Because of the promising research described above, ERIM began, in 1974, to relate grain size, degree of sorting, composition, and water content of beach sands to the spectral properties in the visible, reflective infrared, and thermal infrared regions. The objective was to find quantitative relationships between the spectral reflectances of beaches and their physical properties. During the first two years of the program, 50 beach sand samples from a variety of environments were collected. These samples were analyzed in terms of mineralogy, grain size, degree of sorting and degree of iron staining. In addition the spectral reflectance of each was determined in the 0.35 to 2.5 μm range using the Cary 14 spectrophotometer. A number of different moisture contents were used to simulate different regions in the land/water interface. Thermal infrared measurements were made in the 8-14 μm band on some of the sand types, however, further analysis was restricted to visible and near IR wavelength because of moisture attenuation in this region.

Several regression equations were developed at the end of the second year in an effort to predict grain size and moisture from spectral data. Among them, a two channel moisture algorithm was developed which resulted in a coefficient of variation, R^2 of 0.79 and a standard error of 4.5%. Another moisture algorithm that used five spectral channel ratios was capable of predicting moisture content with a standard error of 4.0% and a R^2 of 0.86. For grain size, one algorithm using 10 ratios was found capable of predicting

the Wentworth grade scale of beach sands with an R^2 of 0.83. Although the results appeared very good, the physical reasoning for the spectral channel selection and success of these algorithms was felt to be somewhat in doubt. In addition the large number of factors in the regression coupled with the relatively small data set reduced the significance of the results. These equations did, however, show the feasibility of developing an algorithm which could successfully predict moisture and grain size from spectral data.

In order to better control the variable parameters of beach sands and to more economically create the necessary data sets, work began in the third year on an adaptation of the Suits radiative transfer vegetative canopy model to the beach sand situation. The initial model, SANDREF, was verified by the end of the third year on two dry sands; a carbonate type and a pure quartz type. In the process of developing this unique modeling approach, the scattering coefficient (s), forward scattering (FS), and absorption coefficient (a) of sixteen common beach forming minerals were derived. This was the first time such a measurement had been achieved for these minerals. In order to develop these parameters three thin sections of each mineral of interest had to be cut. Each section had to be slightly thinner than the one before it. Using the reflectance and transmittance of each of the three thin sections, an iterative curve fitting procedure was used to develop the a, FS, and s parameters. These parameters were then used to predict the reflectance and transmittance of a given mineral at any desired thickness. The reflectance and transmittances were then entered into the SANDREF model.

After SANDREF was proven to work, it was modified to utilize moisture input to simulate the spectra of sand which contains water. The new program, called AQUASANDREF, included a moisture algorithm. The two modeling programs were then combined at the beginning of the fourth year into a single all-purpose program called AQUASAND

(Shuchman, et al., 1978). This composite program can theoretically handle any beach sand situation. It should be stated that the AQUASAND model is not designed to predict sand parameters from reflectance spectra but rather to generate spectra from known parameters. These spectra, in conjunction with measured spectra may be used to generate a predictive algorithm.

Specifically, during year four a new method of modeling the iron stain frequently found as a coating on sand grains was developed, the two models, AQUASANDREF and SANDREF, were combined and shortened into a much more efficient form (AQUASAND) for beach sand modeling. This version handled modeling for both wet and dry sands, and a total of seven diverse beach types were modeled successfully using separate mineralogical and moisture inputs to the AQUASAND model. This work leads into the research reported in this report: the development of a mineralogy, moisture and grain size algorithm, and the verification of this model on laboratory and aircraft produced data.

3

MOGS ALGORITHM

Through the use of the AQUASAND model, we were able to generate the spectral signature of beach sands by varying the mineralogy, moisture and grain size. The goal of this study was to reverse the AQUASAND model, i.e., given the reflectance spectrum of a sand sample, generate the mineralogy, grain size, and moisture of that sample. This section will discuss the development of such an algorithm.

Examples of actual versus AQUASAND generated spectra are given in Figure 1. From inspection of these examples, one can see the ability of the AQUASAND model to closely predict the spectra of certain beach sands. Further examination of the beach sand spectra revealed that the mineralogy had by far the greatest influence on bulk reflectance. So great is this influence that it tends to mask the more subtle features of changes in grain size and, to a much lesser extent, moisture. It was decided that in order for the algorithm to handle a broad variety of sand types and still maintain the resolution needed to detect small spectral features, a preprocessing classification of mineralogy would be necessary.

In order to discriminate mineralogy, a vector length decision framework was used. The concept is developed as follows.

Suppose that there are two points, A and B, located in two dimensional space. The distance, or vector length, L, from A and B can be expressed in terms of the X and Y coordinate locations of points A and B as:

$$L = (X_A - X_B)^2 + (Y_A - Y_B)^2. \qquad (1)$$

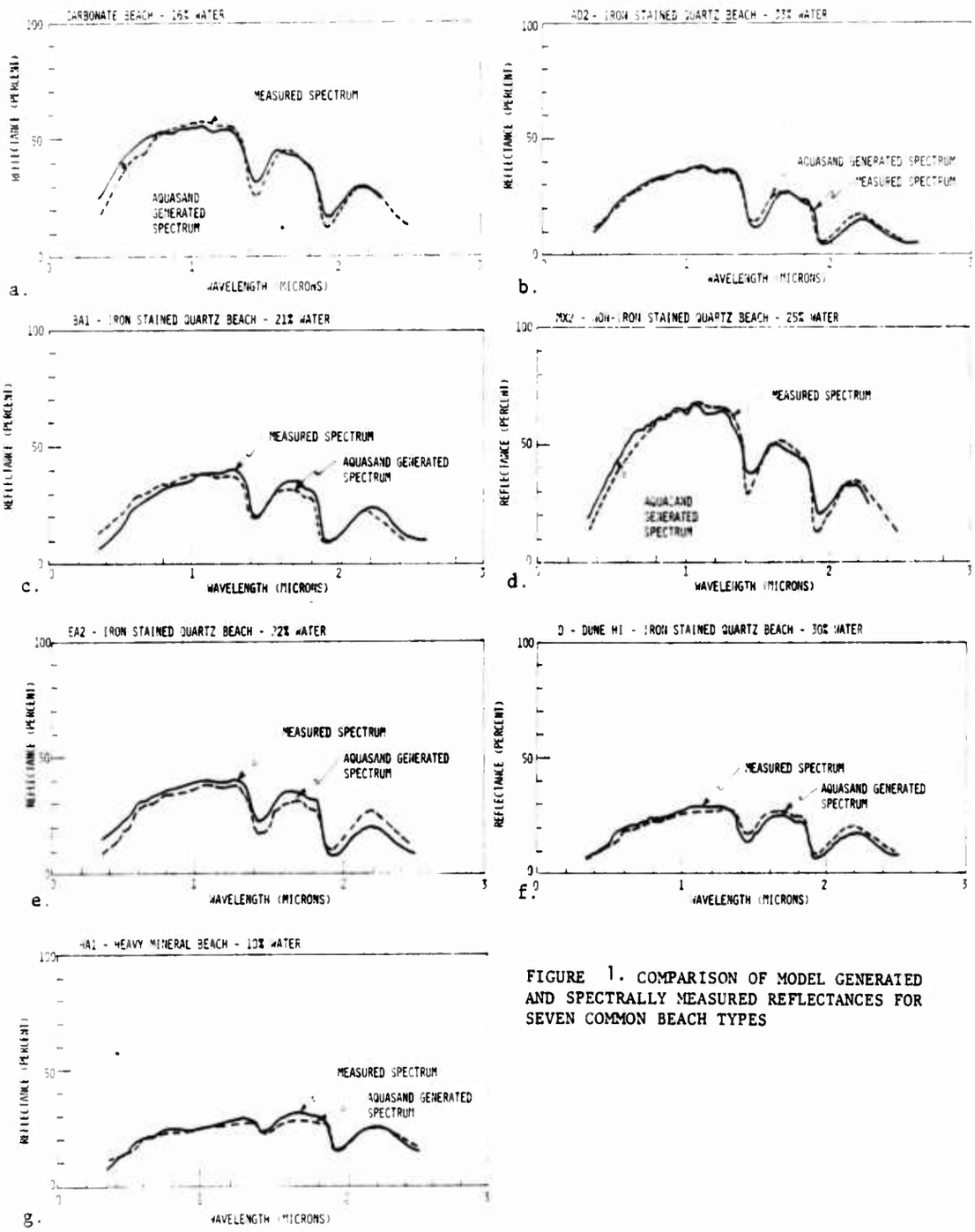

FIGURE 1. COMPARISON OF MODEL GENERATED AND SPECTRALLY MEASURED REFLECTANCES FOR SEVEN COMMON BEACH TYPES

This is, of course, related to the Pythagorean Theorem. Now suppose we have a p-dimensional system with A and B located in each dimension. the vector length can be expressed as

$$L = \sqrt{\sum_{i=1}^{p} (X_{iA} - X_{iB})^2}, \tag{2}$$

where X_{iA} is the location of point A in the ith dimension and X_{iB} is the location of point B in the ith dimension.

This rationale can be used to classify some point, T, as being the member of one of n classes (A_j, j = 1,n), by finding the minimum vector length from T to A_j(j = 1,n). In other words T is said to be a member of the class which is closest to it, on the average across all p dimensions. The minimum vector length is defined as

$$L_{min} = \min_{j=1,\ldots,n} \sqrt{\sum_{i=1}^{p} (X_{iT} - X_{iAj})^2} \tag{3}$$

Notice that equation 3 has no provision for variability in the n classes, therefore, L_{min} is chosen as being the shortest linear vector length. If each class has the same variability associated with it, this causes no difficulty. In this experiment, however, there were considerable differences in variability between the classes so that a modification of equation 3 had to be made. The standard deviation (SD) was used to modify the distance between T and Aj related to each dimension thus removing the effects of variability from each class. This normalized minimum distance equation is expressed as

$$L_{min} = \min_{j=1,\ldots,n} \sqrt{\sum_{i=1}^{p} (X_{iT} - X_{iAj})/SD_{ij}}^2, \tag{4}$$

where SD_{ij} is the standard deviation associated with the j^{th} class in the ith dimension.

In the application of this method to the classification of mineralogy, the "dimensions" are spectral bands or ratios of spectral bands and the "classes" are mineralogical types. Eight spectral bands (Table 1) and all possible unique ratios of those spectral bands were used to classify the mineralogical type of an input sand as one of five categories (Table 2). The object was to make each category as homogeneous as possible so that the moisture and grain size regressions which followed would be sensitive to small scale spectral changes.

Using the AQUASAND model we found that information related to moisture content of sands is best derived from the spectral region beyond 1.0 μm. This is due to the fact that the spectral reflectance of sand in this region is reduced by absorption in proportion to the amount of water present. Exceptionally high spectral absorption is noted near 1.4 and 1.9 μm. Although the spectral reflectance in these regions is highly correlated to moisture we did not consider them since atmospheric absorption prohibits their use by an airborne sensor.

Changes in grain size seem to manifest themselves most clearly in the shorter wavelengths (.4-.7 μm). Grain size information is gained by light being reflected from sand grains below the surface through surface grains. The transmittance through the surface grains is reduced by internal scattering and absorption of the particle. Since both of these factors are dependent on thickness, the bulk reflectance of a sand is dependent to some degree on the grain size.

Table 1. The 8 spectral bands used in the breakdown of beach mineralogy into 1 of 5 categories. In addition to these 8 bands all unique ratio combinations were also used.

Band #	Wavelength Range (μm)
1	.43-.47
2	.47-.49
3	.51-.53
4	.53-.56
5	.59-.63
6	.80-.90
7	.90-1.0
8	1.0-1.1

Table 2. The 5 potential mineralogical classifications

Class #	Description
1	Iron stained Atlantic coast type
2	Iron stained Michigan coast type
3	Iron stained pure quartz type
4	Heavy mineral type
5	Carbonate type

Theoretically a large grain sand should have a lower reflectance than a small grain sand of the same mineralogical composition and with similar moisture content. According to our measurements this appears to be the case.

This grain size phenomenon can be confounded in two ways. First if there is no scattering or absorption within the grains (i.e., a perfectly clear material at all wavelengths) there can be no attenuation. Fortunately, even in our purest quartz sands there were enough impurities and inclusions to give some attenuation. Second, the sand grains may be opaque and thus attenuate too much light. This appears to be the case in the heavy mineral and carbonate beaches. Most of the bulk reflectance for these two types was due to surface reflectance and little if any was due to light transmitted through the surface grains from below. We were unable to create accurate grain size equations for these types.

Utilizing the physical phenomena discussed above we were able to develop multiple linear regression equations for predicting moisture in all five mineralogical classes and grain size for three of the five mineralogical classes. The basis for all the regressions except one was the sample group corresponding to a given mineralogical class. The single exception was the grain size equation corresponding to a pure quartz beach. Our samples within this type consisted of a single grain size (0.22 mm) and, as such did not provide an adequate basis for regression equations. For this case we used AQUASAND generated spectra to simulate a wide range of grain sizes in order to add grain size variability to the data set.

Seventeen spectral bands between 0.4 and 2.5 μm were chosen for use in the regressions (Table 3). Within the 17 bands, only those which were predicted by the AQUASAND model to be most informative were used. In this way we could be reasonably certain that the regression equations would respond the correct parameter and thus yield accurate

Table 3. The 17 bands used in the development of moisture and grain size regression equations

Band #	Wavelength Range (μm)
1	0.43-0.47
2	0.47-0.49
3	0.49-0.51
4	0.51-0.53
5	0.53-0.56
6	0.56-0.59
7	0.59-0.63
8	0.63-0.67
9	0.70-0.75
10	0.75-0.80
11	0.80-0.90
12	0.90-1.00
13	1.00-1.10
14	1.10-1.20
15	1.20-1.35
16	1.50-1.85
17	2.10-2.50

predictions. The predictive equations together with the associated standard errors (SE), and coefficient of variation (R^2) are given in Table 4.

In summary the MOGS algorithm (Figure 2) represents a computer controlled package of equations. The input is a set of 17 spectral reflectance bands obtained from an unknown sand. Based on these bands, the sand is classified as being a member one of five mineralogical types. Depending on the mineralogical type, the appropriate moisture and grain size (where applicable) equations are applied to the data. The output from the MOGS algorithms is the predicted mineralogical class, the predicted moisture, and the predicted grain size.

Table 4. Multiple linear regression equations for the prediction of moisture and grain size. The equations are listed by mineralogical class. Grain size is in mm.

a. Iron stained quartz - Atlantic coast

$$\text{Predicted moisture \%} = 67.964 - 65.046 \left(\frac{\text{Band 16}}{\text{Band 14}}\right)$$

S.E. = 3.08%, R^2 = 0.888

$$\text{Predicted grain size} = 6.87 - 3.4634 \,(\text{Band 7})^{1/4} + .0300\,(\text{Band 1}) + .01672\,(\text{Band 15})$$

S.E. = 0.13 mm, R^2 = 0.603

b. Iron stained quartz - Michigan coast

$$\text{Predicted moisture \%} = 60.149 - 49.961 \left(\frac{\text{Band 16}}{\text{Band 11}}\right) - 2.226 \left(\frac{\text{Band 17}}{\text{Band 1}}\right)$$

S.E. = 2.56%, R^2 = .970

$$\text{Predicted grain size} = 0.6405 - 0.0152\,(\text{Band 5}) - .0047\,(\text{Band 17})$$

S.E. = 0.055 m, R^2 = 0.558

c. Non-Iron stained quartz

$$\text{Predicted moisture \%} = 127.02 - 65.159 \left(\frac{\text{Band 16}}{\text{Band 15}}\right) - 64.054 \left(\frac{\text{Band 15}}{\text{Band 14}}\right)$$

S.E. = 2.12%, R^2 = 0.971

$$\text{Predicted grain size} = 1.158 - 2.328\,(\text{Band 10}) + .3201 \left(\frac{\text{Band 7}}{\text{Band 1}}\right) + 0.2858\,(\text{Band 16})$$

S.E. and R^2 not applicable

d. Carbonate

$$\text{Predicted moisture \%} = 596.28 - 642 \left(\frac{\text{Band 14}}{\text{Band 17}}\right) - 1.081\,(\text{Band 14}) + 0.1538\,(\text{Band 17})$$

S.E. = 4.09%, R^2 = .879 No grain size equation

e. Heavy mineral

$$\text{Predicted moisture \%} = 19.284 + 11.194 \left(\frac{\text{Band 14}}{\text{Band 17}}\right) - 1.081\,(\text{Band 14}) + 0.1538\,(\text{Band 17})$$

S.E. = 4.09%, R^2 = .879 No grain size equation

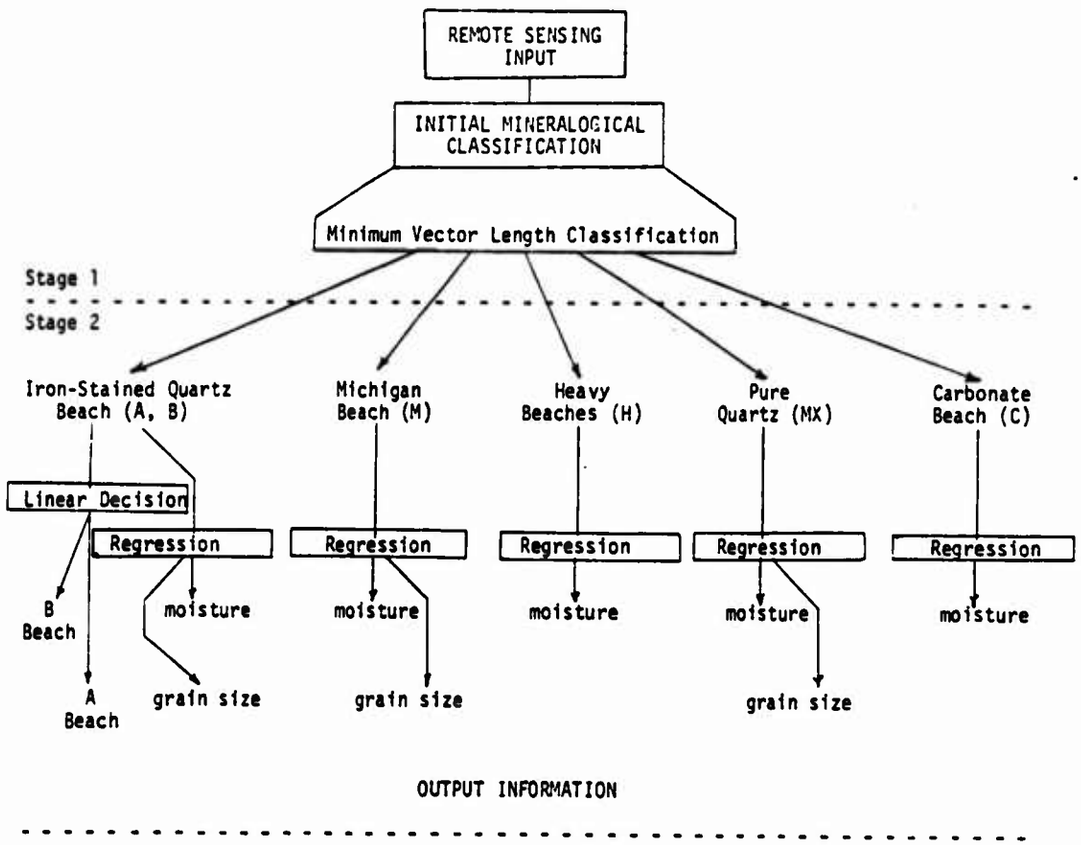

FIGURE 2. FLOW DIAGRAM OF THE MOGS ALGORITHM.

4

MOGS ALGORITHM TESTS

It is recognized that the MOGS algorithm was generated from a very limited data set. It is, therefore, necessary to test this model before a decision is made on its usefulness. Not surprisingly, when the sand samples from which the algorithm was developed were used to test the model, very good results were obtained. This, however, was expected. To realistically evaluate the model, more rigorous tests had to be conducted.

Not only should other laboratory generated sand spectra be tested, but the use of this algorithm on multispectral scanner collected data also needed to be evaluated. This section deals with two such tests.

4.1 LABORATORY TESTS

Six unknown (to the technician conducting the tests) sands were collected for use in testing the MOGS algorithm under laboratory conditions. Three of these sands were from Atlantic Coast quartz beaches, two were from carbonate beaches and one was from a Michigan quartz beach. Each sample was subdivided into subsamples. These subsamples were mixed with varying, known amounts of water to create different moisture conditions.

The spectra of these subsamples were next measured using a Beckman spectrophotometer. The output from the Beckman were in analog form; therefore, the data had to be digitized. Considerable software development was necessary to transform the digitized data into a form which was compatible for input into the MOGS algorithm.

Table 5 summarizes the results for the sand samples analyzed in the laboratory. Given in this table are the sample number, the sand identification (actual and predicted) the percent moisture (actual and

Table 5. Comparison of Actual Sand Parameters to Predicted Classification by the MOGS Algorithm

Sample	Sand I.D.		Moisture %		Grain Size (mm)	
	Actual	Predicted	Actual	Predicted	Actual	Predicted
1a		MICH	3.0	1.1	.38	.46
1b		MICH	10.0	11.6	.38	.48
1c		MICH	19.0	24.5	.38	.48
1d		MICH	26.0	36.3	.38	.49
2a		MICH	2.0	0	.71	.29
2b		MICH	11.0	11.1	.71	.45
2c		MICH	17.0	28.0	.71	.50
2d		MICH	29.0	31.2	.71	1.04
3a	CARB	CARB	2.0	0	---	---
3b	CARB	CARB	15.0	14.0	---	---
4a		MICH	5.0	1.2	.21	.48
4b		MICH	12.0	9.0	.21	.47
4c		MICH	20.0	23.6	.21	.48
4d		MICH	25.0	35.3	.21	.51
5a	CARB	CARB	8.0	10.1	---	---
5b	CARB	CARB	20.0	23.3	---	---
6a	MICH	MICH	37.7	25.6	.26	.28
6b	MICH	MICH	3.2	3.7	.28	.30
6c	MICH	MICH	0.3	0.0	.25	.32
6d	MICH	MICH	12.1	16.0	.23	.29
6e	MICH	MICH	15.0	17.7	.25	.30
6f	MICH	MICH	28.0	26.2	.28	.29

predicted) and the grain size (actual and predicted). We can see that the MOGS algorithm correctly identified the mineralogy only 50 percent of the time. The reason for this is two-fold. First, the MOGS algorithm was developed using a very limited number of beach sand samples. Therefore, when confronted with a sand which has a very different composition from those used in the development of the model, the MOGS algorithm has difficulty classifying that sand. Secondly, the instrument which originally measured the sand samples for development of the MOGS algorithm was a Cary-14 spectrophotometer. The instrument used to measure the test samples was a Beckman spectrophotometer. While these two instruments operate using the same principle, and produce quite similar results, it is possible that these instruments would give two different reflectances for the same sample over very narrow wavelengths. We can see from Table 1 that many of the bands used in the mineralogy classification are narrow bands; a small variation in the location of these bands between the two instruments could result in a misclassification.

The moisture results were quite good. The correlation of predicted to actual moisture is 0.93 (significant at the 0.01 level). The moisture predictions, however, appear suspect at higher moistures.

The grain size predictions were quite poor for the laboratory examples. This is in part due to the MOGS algorithm's misclassification of the mineralogy of half the examples, and in part to the limited number of samples used in developing the algorithm.

4.2 MULTISPECTRAL SCANNER TESTS

The MOGS algorithm was tested on two separate sets of ERIM collected multispectral scanner data. One set, collected at Panama City, Florida, was obtained before the development of the MOGS algorithm, and only contained enough spectral bands of data to provide a moisture map of the test area. Data collected over a Lake Michigan

test site was obtained during the development of the MOGS algorithm and contained the proper spectral bands for the MOGS algorithm.

4.2.1 PANAMA CITY TEST SITE

Multispectral scanner (MSS) data from the morning of 23 April 1976 was interpreted to be the best available from the Panama City test site for input into the MOGS algorithm. Unfortunately, none of the Panama City collected data contained enough spectral bands for grain size analysis. Additionally, of the three spectral bands needed for the moisture equation (see Table 4) only two were available, and thus the moisture algorithm had to be modified accordingly.

Figure 3 shows the moisture map for the Biltmore Beach test site. The Biltmore Beach is a typical coastal beach in that it is well drained, and on a sunny day like the one when the data was collected, the surface layer of sand is virtually moisture free.

4.2.2 LAKE MICHIGAN TEST SITE

The ERIM MSS was flown over a portion of the Lake Michigan shoreline near Pentwater, Michigan on 1 November 1978. ERIM scientists were present during this time, collected samples were for laboratory analysis of grain size and moisture content. The MOGS algorithms was modified to conform to the 12 band configuration of the ERIM scanner used during this data acquisition.

The actual and MOGS predicted moisture and grain size data for the field collected samples are presented in Table 6. The agreement between the actual and the MOGS predicted parameters appear to be quite good, but the moisture prediction appears particularly poor for high moisture contents. This may be due to the fact that wet sand at the test sites appeared to exhibit bi-directional dependencies (i.e., a failure to behave in a Lambertian manner). These bi-directional characteristics are enhanced at low sun angles and are not accounted

a. MSS Image (.80-.90) of Biltmore Beach Area

b. Moisture Distribution

FIGURE 3. DIGITAL IMAGERY GENERATED BY THE MOGS ALGORITHM, SHOWING MOISTURE DISTRIBUTION AT BILTMORE BEACH, PANAMA CITY, FLORIDA. (White areas are either unclassified regions or open water areas.)

Table 6. Comparison of actual parameters to predicted classifications by the MOGS algorithm. The sand spectra used here were collected by the ERIM MSS

Sample Mineralogy		Moisture %		Grain Size (mm)	
Actual	Predicted	Actual	Predicted	Actual	Predicted
MICH1	MICH	22.3	12.1	.25	.32
MICH2	MICH	1.0	0.0	.23	.28
MICH3	MICH	8.0	10.1	.22	.25
MICH4	MICH	28.0	16.9	.26	.35
MICH5	MICH	5.0	2.2	.24	.26

for by the MOGS algorithm. Although the flight took place at 1:30 EST the sun was only 38° above the horizon on November 1. To minimize bi-directional reflectance variations, future aircraft flights should be made during complete mid-altitude (3000 m) cloud cover or sunny skies with the sun close to the zenith (summer sun).

Applying the same moisture and grain size equations used in the previous analysis, the entire Pentwater State Park beach on a pixel by pixel basis (in this case 1.5 x 1.5 meters) was classified with respect to grain size and moisture content. The two MOGS generated digital maps (see Figure 4) show the predicted moisture and grain size distributions on the beach at Pentwater. The ground truth measurements taken at the time of flight correlate well with these images. Figure 4 helps to demonstrate how an entire sandy coastline could be analyzed in respect to moisture, grain size, and gross mineralogy using a small subsection as calibration.

MOISTURE DISTRIBUTION IMAGE - LIGHTER SHADE INDICATES HIGHER MOISTURE CONTENT

0-5% 5-20% 20+%

GRAIN SIZE DISTRIBUTION IMAGE - LIGHTER SHADE INDICATES LARGER GRAIN SIZE

.15-.25 mm .25-.40 mm >.40 mm

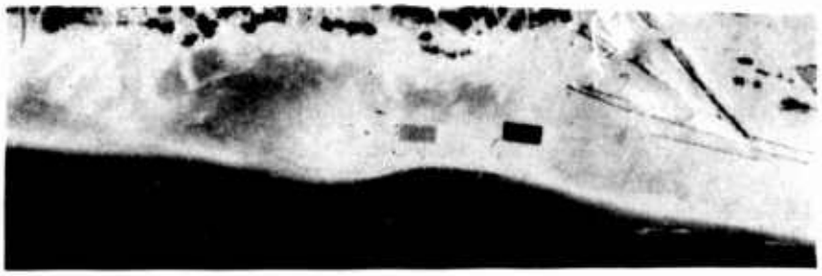

PANCHROMATIC AERIAL PHOTOGRAPH

FIGURE 4. DIGITAL IMAGERY, GENERATED BY THE MOGS ALGORITHM SHOWING THE DISTRIBUTION OF MOISTURE AND GRAIN SIZE ON PENTWATER BEACH (PENTWATER STATE PARK, MICHIGAN). WHITE AREAS ARE EITHER UNCLASSIFIED REGIONS OR OPEN WATER.

5

USE OF SATELLITE MULTISPECTRAL SCANNER DATA AS MOGS ALGORITHM INPUTS

Based on the parameters of current spaceborne (MSS) systems and the specific requirements of the MOGS algorithm, there appears to be very limited potential in using satellite data as inputs into the algorithm. This is based on two observations: (1) the present number of spectral bands available on satellite multispectral scanners are limited to three or four, where the MOGS algorithm currently needs a large number of spectral bands to operate; and (2) the resolution of spaceborne scanner systems are probably too coarse to image beach environments.

The MOGS algorithm was derived using eight bands of information for the initial mineralogical classification. After this, up to six more bands were needed to produce the moisture and grain size predictions. Current satellite systems (i.e., the Landsat series) have only four channels of information (see Table 7). From Table 7, it can be seen that future proposed satellite systems will have more channels than the existing Landsat series. But even the six channels of data which both Landsat-D or CZCS will have do not come close to matching the 14 channels of data the MOGS algorithm needs. Given the marginal manner in which the MOGS algorithm performed, given all of the information it needed, it is doubtful it could effectively perform with even less information.

Beach environments of the type being studied in this investigation (bare soil, no vegetation) are typically no wider than one to two hundred meters. given the pixel size of current satellite MSS systems (approximately 80 meters), it is unlikely that more than two or three pixel wide strip of information could be obtained. This would be of very little use in beach trafficability modeling. The improved resolution of the Landsat-D and SPOT systems offer the potential to better

Table 7. Spectral Parameters

MOGS Algorithm	Landsat 1-3	SPOT	Landsat-D	CZCS*
0.43-0.47				0.42-0.44
0.47-0.49			0.45-0.52	
0.49-0.51				
0.51-0.53	0.5-0.6	.50-.59		0.50-0.5
0.56-0.59			0.52-0.60	0.53-0.5
0.59-0.63				
0.63-0.67	0.6-0.7	.61-.69	0.63-0.69	0.65-0.6
0.70-0.75				
0.75-0.80	0.7-0.8		0.76-0.90	0.73-0.7
0.80-0.90		.79-.90		
0.90-1.00	0.8-1.10			
1.10-1.20				1.148-1.152
1.20-1.35				
1.50-1.85			1.55-1.75	
2.10-2.15			2.08-2.35	

Spatial Resolution

ERIM MSS8 Scanner	Landsat 1-3	SPOT	Landsat-D	CZCS*
3 m x 3 m	57 m x 79 m	20 m	30 m x 30 m	825 m x 825 m

*Coastal Zone Color Scanner

discriminate beach environments, while the coarse resolution of the CZCS system offers virtually no potential.

Also to be considered in using satellite systems is the timeliness of the data. Currently, data from a specific area is only available once every several days. The data then has to be corrected for atmospheric effects. In summary, it is felt that there is very little potential for using satellite collected data in beach environment modeling given todays operational MSS satellites.

6

APPLICATION OF A MOGS TYPE ALGORITHM TO NON-SAND SOILS

This section of the report discusses modeling of non-sand soils. Specifically, the question addressed is whether a MOGS type algorithm could be applied to mud flats where the water to particle volume ratio is very high.

There are two important assumptions required by the reflectance model of moist beach sands and natural water bodies. First, one assumes that the air-water or air-sand boundary is essentially planar. In the case of beach sands, this planar surface is obtained naturally by wind on dry sand or by rain and wave action on wet sand. Gravity maintains a planar surface on water except at high sea states when the model reflectance predictions will begin to deviate from field measurements. On the other hand, soils containing silt and clay can sustain a non-planar macrostructure of the wet or dry surface. This macrostructure will tend to alter the directional properties of reflectance by significant amounts. Although spectral variations will be the same, the magnitude of reflectance in a given direction will change.

Second, soils containing silt or clay tend to compact with various kinds of microstructures depending upon soil history. A basic model assumption concerning the scattering of radiation by particulates is that the particulates are randomly distributed throughout each stratum. Optical contact between particulates is assumed to have negligible effect in the scattering process. In the case of sand, the microstructure is assumed to be a random stacking with the area of points of contact between grains negligibly small compared to particulate surface area. In this regard, all sands have a similar microstructure and the points of contact do not influence

PRECEDING PAGE BLANK-NOT FILMED

the scattering significantly. In saturated sands, the scattering is fundamentally the same as that of a very turbid natural water body, so turbid with sand that the particulates rest upon each other and occupy a major fraction of the volume of the water body. As water is drained to field capacity, air is drawn into the void spaces but a continuous film of water surrounds each sand grain. The model treats the air in the voids as merely a new kind of scattering particulate in the turbid water with a total volume equal to the total volume of air in voids and a concentration equal to the number of voids per unit sand volume. The number and size of voids will be directly related to the number and size of sand grains which make these voids by random packing.

In some soils containing clay, the void spaces may be made as a result of preferential platelet to platelet stacking induced by the surface tension of the water adhering to the particulates. Therefore, the size of voids will be microstructure dependent. In addition, the areas of optical contact between particulates may be a large fraction of the area of a particulate and thereby favor optical transmission from particulate to particulate through very thin water interfaces instead of scattering through water and air voids to arrive at the next particulate as in sands. The net effect will be a scattering process similar to that for a much larger particulate than the individual clay particles. The size of this composite particulate will be microstructure dependent.

The proper modeling of planar surfaces of soils would require that this microstructure be taken into account. Although the spectral features would be predicted correctly by the present sand model, the quantitative accuracy as to proportions of water, air, and mineral would not likely be accurate without modification.

The modeling of non-planar soil surfaces requires the introduction of a new driving parameter which describes, in some suitable statistical manner, the variations of the surface from a

plane. In order for a model which incorporates surface irregularity to be useful, it would be necessary to show that the natural soil surfaces of interest become irregular in a relatively few characteristic ways. Otherwise, there would be an unmanagably large number of possibilities for directional reflectance variations depending upon chance.

7

SUMMARY AND CONCLUSIONS

The four year activity summarized in this report represents a significant contribution to the understanding of the spectral reflectance response of beach sands in the .4 to 2.5 μm region of the electromagnetic spectrum. The spectral shape of five mineralogical types were studied in detail and a radiative theory to adequately describe the spectral shapes of the beach sands was developed through the generation of the "Suits AQUASAND" radiative transfer model. This model, an adaptation of a vegetation reflectance model, calculates sand reflectance based on mineralogical inputs and is currently being used by University of Michigan faculty and scientists from the United States Geological Survey.

The final year and one-half of this research program was concerned with development of a methodology whereby an algorithm (the MOGS algorithm) was produced to predict mineralogy, moisture, and grain size of unknown beach sands. The developed MOGS algorithm appeared to work quite well in prdicting the general mineralogy type and moisture of sands similar to the ones used to develop the model, however, difficulties arose when trying to predict grain size and classifying sands different than the ones used to produce the model. It is felt that the shortcomings of the MOGS algorithm could be overcome if a larger number of beach sand samples were used. The basic methodology used to develop the model is believed to be sound and can be used in other remote sensing applications.

One application for the MOGS algorithm was to determine whether or not remote sensing data can be used in beach trafficability models. Prior to the development of the MOGS algorithm, it was believed that grain size and soil moisture were the two most important variables in beach trafficability models. Recent studies (Thomson, et al., 1980) have indicated that this is not entirely true.

PRECEDING PAGE BLANK-NOT FILMED

This later study determined that of all the factors needed to predict a soil penetration resistance (cone index) for a given situation, soil moisture and in situ void ratio were the most important. Grain size was relatively unimportant in the sense that only gross gradation of grain sizes are needed as inputs into the beach trafficability model. It was also reported that the soil moisture required by the beach trafficability model was not a surface moisture, as determined by the MOGS algorithm, but a soil moisture profile over the first 15 centimeters of the sand. The MOGS algorithm produces a soil moisture for the first centimeter of sand at the surface.

The main conclusion with respect to beach trafficability is that in order to use present day beach trafficability models, additional information is needed: a third dimension (depth) of soil moisture data and an estimate of in situ void ratio. Up to the present, neither of these parameters have been studied in detail to ascertain as to whether or not they can be remotely sensed.

Remote sensing's utility in providing trafficability inputs is in providing synoptic and temporal coverage of a given geographic location. A hybrid approach of ground truth test plots coupled with remote sensing data to determine areal extent of a given set of environmental parameters is perhaps the most plausible approach in solving the trafficability input problem.

To summarize the overall four year research activity, it can be stated that remote sensing algorithms using passive .4 to 2.5 μm data have been developed to predict moisture and grain size for a limited class of beach materials. These algorithms can provide useful information for a variety of coastal geographic studies, but inherent limitations of the technique preclude its utilization as a primary data source for beach trafficability predictions.

REFERENCES

Hovis, W.A. and W.R. Callahan, Infrared reflectance spectra of igneous rocks, tuffs, and red sandstone from 0.5 to 22 μm, J. of the Opt. Soc. of Am., Vol. 56, No. 5, pp. 639-643, 1966.

Hunt, G.R. and R.K. Vincent, The behavior of spectral features in the infrared emission from particulate surfaces of various grain sizes, J. of Geophys. Res., Vol. 73, No. 18, pp. 6039-6046, 1968.

Shuchman, R.A., G.H. Suits, and C.F. Davis, AQUASAND: A beach reflectance model and validation tests, paper presented at Fifth Canadian Symposium on Remote Sensing of the Environment, August 26-30, Victoria, British Columbia, Canada, 1978.

Thomson, F., R. Shuchman, K. Knorr, J. Ott, and F. Sadowski, Studies of the utility of remotely sensed data for making mobility estimates using AMC mobility models, ERIM Final Report No. 140300-2-F, Ann Arbor, Michigan, 1980.

Vincent, R.K., Rock-type discrimination from ratio images of the Pisgah Crater, California test site, The University of Michigan, Report No. 3165-77-T, NASA Contract NAS9-9784, 1972.

Vincent, R.K., A thermal infrared ratio imaging method for mapping compositional variations among silicate rock types, unpublished PhD dissertation, The University of Michigan, 1973.

Vincent, R.K., and F.J. Thomson, Spectral compositional imaging of silicate rocks, J. of Geophys. Res., Vol. 77, pp. 2465-2471, 1972.

Vincent, R.K., F.J. Thomson, and K. Watson, Recognition of exposed quartz sand and sandstone by two-channel infrared imagery, J. of Geophys. Res., Vol. 77, pp. 2473-2477, 1972.

Watson, R.D., Surface-coating effects in remote sensing measurements, J. of Geophys. Res., Vol. 75, pp. 480-484, 1970.

APPENDIX

This appendix contains three publications which resulted from work done for this contract. These papers are:

1. "AQUASAND: A Beach Reflectance Model and Validation Tests," published in the Proceedings of the Fifth Canadian Symposium on Remote Sensing of Environment, Victoria, B.C., 1978.

2. "The Use of Remote Sensing in the Determination of Beach Sand Parameters," published in the Proceedings of the Thirteenth International Symposium on Remote Sensing of Environment, Ann Arbor, Michigan, 1979.

3. "Determination of Beach Sand Parameters Using Remotely Sensed Aircraft Reflectance Data," accepted for publication in Remote Sensing of Environment, 1981.

PRECEDING PAGE BLANK-NOT FILMED

AQUASAND: A BEACH REFLECTANCE MODEL AND VALIDATION TESTS*

R.A. Shuchman, G.H. Suits, C.F. Davis
Environmental Research Institute of Michigan
Ann Arbor, Michigan 48107

ABSTRACT

A new sand reflectance model called AQUASAND has recently been developed. This model, a modification of the Suits radiative transfer vegetation canopy directional reflectance model, accounts for the reflectance and transmittance of sand particulates in the .35 to 2.5 μm spectral range. The AQUASAND model also accounts for the influence of soil moisture within the sand. The model will ultimately determine the practical limits of remote sensing algorithms for determining physical and chemical properties of beaches.

The AQUASAND model uses, as inputs, the coefficients of absorption and scattering and the forward scattering fraction for each mineral comprising the beach sand (i.e., quartz, feldspar, kaolinite, etc.), the average number of grains (particles) per given volume from which average cross sections of each mineral type can be computed, void space, and the moisture depth profile of the beach to calculate the reflectance of the beach. ERIM, using its Cary 14 spectral reflectometer, measured the hemispherical transmittance and reflectance of sixteen common beach forming minerals at a number of prescribed thicknesses to obtain the needed coefficients and forward scattering fraction.

Additionally, ERIM used the same instrument to measure actual sand samples collected from fifty diverse beaches found on United States coastlines. These reflectance spectra were used to evaluate the AQUASAND model. The results are very encouraging, showing good agreement between the actual beach spectra and the model results when the individual mineral components comprising the beach are correctly identified and inputed into the model.

The validated AQUASAND model (based on ten of the fifty actual beach samples) is currently being used to generate algorithms that predict grain size, moisture contents, and mineral composition using remotely sensed reflectance information in the .35 to 2.5 μm spectral range.

*This work is supported by the United States Office of Naval Research (ONR), Contract No. N0014-74-0273. Dr. Hans Dolezalek is the technical monitor.

Presented to the 5th Canad
Remote Sensing, Victoria,

RESUME

Un nouveau modèle du facteur de réflexion des plages, dénommé AQUASAND, a été mis au point récemment. Ce modèle qui est une variante du modèle SUITS du facteur de réflexion directif du transfert de rayonnement du couvert végétatif, prend en compte les facteurs de réflexion et de transmission des particules de sable dans l'intervalle spectral de 0.35 à 2.5 μm. Ce modèle prend également en considération l'effet de l'humidité dans le sable. Le rôle de ce modèle est de déterminer en définitive les limites pratiques des algorithmes de télédétection servant à établir les propriétés physiques et chimiques des plages.

Les données d'entrée introduites dans AQUASAND pour le calcul du facteur de réflexion des plages sont: les coefficients d'absorption et de diffusion, ainsi que la fraction de pro-diffusion de chacun des minerais entrant dans la composition du sable de plage (quartz, feldspath, kaolinite, etc.); le nombre moyen de particules par unité de volume, donnée que l'on utilise pour calculer la section de chaque type de minerai; l'espace des vides; et la répartition en profondeur de l'humidité. ERIM, au moyen de son réflectomètre spectral Cary 14, a mesuré le facteur de transmission hémisphérique et le facteur de réflexion de seize des principaux minerais entrant dans la composition des plages, à des épaisseurs prescrites pour déterminer les coefficients indispensables et la fraction de pro-diffusion.

En outre, ERIM s'est servi du même instrument pour étudier des échantillons de sable prélevés dans cinquante plages différentes des littoraux américains. Les spectres du facteur de réflextion obtenus ont été employés pour apprécier le modèle AQUASAND. Les résultats sont très encourageants; il y a un accord très bon entre les spectres de plage réels et les résultats simulés quand les minerais individuels constituant la plage sont bien identifiés et introduits dans le modèle.

Le modèle AQUASAND validé (reposant sur 10 des 50 échantillons de plage réelle) est utilisé régulièrement pour élaborer des algorithmes qui prédisent la granulométrie, les teneurs en humidité et la composition en minerais, en se servant du facteur de réflexion télédétecté dans l'intervalle du spectre compris entre 0.35 et 2.5 μm.

1.0 INTRODUCTION

This paper discusses a new radiative transfer model called AQUASAND. This model predicts the reflectance of beach sands in the .35-2.5 μm wavelength range of the electromagnetic spectrum. This newly developed sand

Appendix-B MI-3 EBIR Image Annotation (cont.)
(Second line of annotation)

(annotation)	(description)
POSITION ERROR 10.00 KM	
	-- the position error root mean square of the scene is less than 10 Km.
IMAGE DATA GENERATED 08 AUG 78	
	-- date the master positive film was generated
FC	-- denotes frame centre
C 51- 26- 3	-- C denotes LANDSAT-3 WRS track #51, WRS frame #26, WRS cycle #3. (ref.(6))
TR 5D	-- track number using old ('72-73) tracking system
NTS 92G	-- 1:250,000 NTS map that the image centre is located on.

(The large character annotation)

(annotation)	(description)
C 51- 26- 03	-- WRS frame number (as above) (ref.(6))
866-A---	-- EBIR frame number 866, WRS sub-frame "A".

reflectance model will ultimately determine the practical limits of remote sensing algorithms for determining physical and chemical properties of beaches.

The use of .35 to 2.5 μm radiation to determine physical and chemical properties of beaches is deemed feasible from the proven capability of mapping silicate minerals using reststrahlen techniques in the 8 to 14 μm spectral range, a procedure developed by Vincient and Thomson (1972) and earlier by Vincient and Hunt (1958). The .35 to 2.5 μm region of the spectrum is of interest for beach parameter sensing since water is relatively transparent in this region (unlike the 8 to 14 μm region) and beaches typically have high moisture contents.

2.0 MODELING

The capability of determining important physical properties of beach sands by remote sensing techniques depends upon the interaction of radiation with the constituent materials of the beach. Such interaction is certainly complex but, nevertheless, must follow the laws of nature. The purpose of making a mathematical reflectance model of this complex interaction is to achieve insight into the relationship between the remotely received signals and the physical properties of the beach sand that are of interest.

A mathematical model of a physical phenomenon is the result of incorporating the mathematical expressions of the laws of nature as they apply to a complex circumstance so that the conclusions drawn from the assembled expressions correspond to the physical results of an experiment under similar circumstances. Such a model requires experimental validation using a few but diverse circumstances in order to prove that the essence of the phenomenon is contained in the logic of the model. Once validation has been achieved, the model may be used as a readily available and inexpensive substitute for experiments under all circumstances within the scope of the circumstances of the validation experiments. In addition, the logical structure of the model provides the insight into the significant interaction processes so that more general conclusions may be drawn.

2.1 Reflectance Model Concepts

The most elementary model of sand reflectance is the simple plane mixtures model. The model employs the assumptions that all sand particles are opaque and are randomly mixed. The surface of the sand layer exposes sand particles in proportion to the product of their mean cross sectional area and the concentration of the particles in the sand mixture. Thus, the reflectance spectrum of the mixture is predicted to be the area weighted average of the reflectance spectra of the various minerals exposed at the sand surface. Multiple scattering between particles is assumed to be negligible and one surface particle is assumed not to obscure from view an adjacent surface particle.

This elementary model fails to achieve good accuracy because the transmittance of particles in a finely divided state may be quite large and multiple scattering of radiation between particles should be significant. In addition, the packing of grains in layers produces partial exposure at the surface so that line of sight to some particles will depend upon the direction of view. A more complex model is required to account for these effects.

The more complex model which is used in this work employs the identical concepts that are employed by the directional reflectance model for vegetative canopies (Suits, 1972). It may be hard to visualize off-hand that the interaction of radiation with a vegetative canopy is homomorphic with the interaction of radiation with sands because vegetation and sand hardly appear the same to the eye. Nevertheless, the essence of the reflection, transmission, and multiple scattering phenomena is the same concept for the optical parameters of the components that are involved as long as the wavelength is much smaller than the particles.

The first assumption of this model is that the scattering components are distributed more or less uniformly in horizontal layers where the mixture of component types may be different in the various layers. In a corn field, for example, the tassels always appear at the top, green healthy mature leaves appear in a middle layer and necrotic leaves appear usually near the soil. In sands, the action of wind and waves is likely to stratify mineral mixtures vertically and certainly moisture content varies with a vertical moisture profile. The division in layers is done in order to quantify statistically what may otherwise be nearly a continuous distribution.

The second assumption is that the radiation field may be divided into two types of radiant flux — specular and diffuse. The specular flux represents the radiation arriving from the source with rectilinear propagation and passes through the holes, cracks, and voids of the ensemble of randomly packed components without deviation. The diffuse flux is derived from the specular flux and is that part of the specular flux which has been intercepted by a scattering component at least once and is scattered in both forward and backward directions. In a vegetative canopy, specular flux frequently reaches the soil

level and appears as sun flecks on the soil. In a sand, specular flux diminishes exponentially to negligible proportions in only a few millimeters depth. Optically, the sand is infinitely deep. However, the diffuse flux is derived from the specular flux in the identical manner. The diffuse flux may penetrate much deeper into the sand than can specular flux.

The third model assumption is that the manner of scattering by mineral particulates can be adequately represented by replacing each mineral particulate with a set of equivalent Lambertian panels which have the same spectral transmittance and reflectance as does the component. This assumption defines a simplified scattering phase function which permits one to calculate ensemble reflectances in closed form. The form of the scattering phase function becomes significant when single scattering is the dominant phenomenon. Scattering by widely dispersed aerosols in the atmosphere (e.g., smoke and dust) exhibits detailed phase function effects. However, as the degree of multiple scattering increases, the detailed features of the scattering phase function are no longer significant. In both sands and vegetative canopies, multiple scattering effects dominate because of the high density of scattering components.

The fourth model assumption is that the diffuse flux moves generally vertically upward and downward with a Lambertian angular distribution as a first approximation. The reflectance of the ensemble is calculated using the method of self-consistent field with the specular and approximate diffuse flux as the illuminant of components. The ensemble reflectance is not necessarily Lambertian but is only approximately so. Both vegetation and sand meet this approximate criterion.

Because of the homomorphic relationship of radiative interactions with sand and vegetative canopies, the reflectance model previously developed for vegetation is applied to sand with the appropriate component properties for sand minerals substituted for vegetative canopies.

2.2 Optical Properties of Sand Components

The cross section view of a hypothetical sand layer containing two kinds of minerals is shown in Figure 1. The irregular shapes of the sand grains result in some more or less random, loose packing with many voids. These grains are to be replaced by a number of equivalent Lambertian panels which will intercept approximately the same amount of radiant flux as do the actual grains. The spectral reflectance and transmittance of the panels are to be the same as the spectral reflectance and transmittance of the grains. Since these spectral properties may change with grain size or state of division, some means of calculating the appropriate spectral properties is required.

An auxiliary reflectance and transmittance model for mineral thin sections was developed in order to relate the inherent spectral properties which are characteristic of a mineral to the properties of that mineral in any state of division. Three characteristic bulk properties were taken to be sufficient for this purpose — the spectral absorption coefficient, a, the forward scattering fraction, FS, and the scattering coefficient, s.

Radiation which penetrates a mineral may be absorbed and converted into heat energy, depending upon the chemical composition of the mineral. A mineral which is internally homogeneous without inclusions and cracks will transmit radiation passing through it in accordance with the relation,

$$E(x) = E_0 e^{-ax}, \qquad (1)$$

where $E(x)$ is the irradiance on a plane at depth x in the mineral,

E_0 is the irradiance on a plane inside the first surface,

a is the spectral absorption coefficient.

The spectral absorption coefficient will be a function of the wavelength of the penetrating radiation and will depend upon the chemical composition of the mineral. The spectral absorption coefficient is largely responsible for the spectral variations in mineral reflectance and transmittance.

The formation of minerals is a complex natural process so that minerals may not be optically homogeneous. Foreign materials are often formed in the interior of the mineral. Such features as fractures, gas bubbles, small crystals of associated minerals, and grain boundaries of anisotropic crystals create inhomogeneities within mineral bodies. These inhomogeneities reflect or scatter and deviate penetrating radiation from rectilinear propagation. A collimated beam of radiation which propagates rectilinearly through the body of a mineral will be diminished due to such scattering by the relation,

$$E(x) = E_0 e^{-sx}, \qquad (2)$$

where $E(x)$ is the irradiance of rectilinear flux on a plane at depth x,

E_0 is the irradiance of rectilinear flux at the first surface,

s is the scattering coefficient.

The radiation which is scattered will tend to propagate either deeper into the mineral -- forward scatter — and contribute to transmittance or reverse direction and propagate back out of the mineral — backscatter — and contribute to reflectance of the mineral. The fraction of scattered radiation which continues deeper into the mineral is the forward scattering fraction, FS. The fraction of scattered radiation which reverses is then (1-FS). The scattering coefficient and the forward scattering fraction can be spectrally dependent but should not be the primary determinant of the spectral quality of a mineral.

These three optical properties of a mineral, a, s, and FS, are assumed to be independent of the thickness of the mineral. That is, the inhomogeneous structure and chemical composition of a mineral thin section is assumed to be evenly distributed so that a, s, and FS are inherent properties characteristic of the kind of mineral and not the size of the mineral sample.

The auxiliary reflectance and transmittance model for mineral thin sections makes use of these three properties and the index of refraction of the mineral to yield the thin section transmittance and reflectance for any mineral thickness. The value of a, s, and FS for each wavelength must be determined experimentally. However, these properties cannot be determined by direct experiment. Instead, a spectral reflectometer was used to measure the transmittance and reflectance of mineral thin sections having various thicknesses. Since a, s, and FS are presumably thickness invariant, the value of a, s, and FS may be determined by finding the value of a, s, and FS which, when used in calculating the transmittances and reflectances of thin sections having these various thicknesses, yield matching values for the reflectances and transmittances found experimentally. A computer iteration technique was used for this purpose.

The spectral values of a, s, and FS for some of the common sand minerals have been tabulated. For certain opaque minerals, such as hematite and limonite, the values of a, s, and FS could not be determined. The transmittance and reflectance of these minerals are independent of grain thickness for all thicknesses that are likely to be found in sands. The reflectance and transmittance of pure, unstained clear quartz is due almost entirely to surface effects which are also independent of grain thickness.

The optical properties of sand components are determined and are introduced into the sand reflectance model. The spectral transmittance and reflectance of the equivalent Lambertian panels for each mineral are determined using the auxiliary reflectance and transmittance model for mineral thin sections where the thickness of thin section is the mean grain thickness for each mineral. The mean cross section of grains of each mineral type is multiplied by the corresponding number of such grains per unit volume for a given beach sample and represents the scattering effect of the equivalent Lambertian panels.

2.3 Model Description

Figure 2 indicates the flow of information beginning with the raw experimental CARY transmittance (τ) and the reflectance (ρ) data and ending with the predicted reflectance spectrum for sand. As indicated previously, the needed inputs into the AQUASAND model are transmittance, τ, and reflectance, ρ, values for the individual minerals in a particular sand configuration. These τ and ρ values must be calculated for each particle size. Experimentally, τ and ρ spectra were determined for each mineral at given thicknesses. Some minerals which were opaque exhibited a negligible amount of transmittance. Iron stains were treated as separate minerals and experimental τ and ρ spectra were determined for them. These inputs are shown on Figure 2.

In order to predict τ's and ρ's for any particle size, properties independent of size can determined. These properties, previously discussed, are the forward scattering (FS), scattering coefficient (s) and the spectral absorption coefficient (a). The computer program calculates these coefficients for a given mineral using the experimental τ's and ρ's and the experimental thicknesses and the parameters of refraction (particle to air (RPA) and air to particle (RAP)).

These determinations of the fundamental a, FS, and s properties of sixteen common beach forming minerals in the .35-2.5 μm range are the first such measurements made to date. Figure 3 is a plot of a (α) and s for a carbonate beach.

Once the absorption and scattering coefficients are determined, another computer program uses these coefficients coupled with the parameters RPA and RAP to predict τ's and ρ's for a given thickness. These predicted values are then used to model the sand.

The final program, AQUASAND, computes the reflectance of mixtures of minerals. The inputs to this program consist of the predicted τ's and ρ's for the minerals constituting the sand, the amount of iron stain, the depth of the sand, the reflectance of an infinite depth background underneath the sand, the particle cross sections and packing factors for the various minerals, the angle of illumination

from a point source illuminator (or optional Lambertian source) and the angular position of the sensor and the percent moisture of the sand on a millimeter scale.

The output of AQUASAND is a predicted reflectance spectra of the sand for various configurations of illuminator position (Θ) and sensor position (Φ, Ψ). The AQUASAND program was derived from a program which predicted reflectances for a two layered vegetation canopy with a background. Thus the sand can have two layers with different densities and grain sizes in each layer. A background material for the sand can also be specified. These properties of AQUASAND allow great flexibility for modeling various configurations such as thin sands, sand after a storm with a layer of organic matter or stones on top, etc.

3.0 RESULTS

Seven beaches of diverse mineralogy, moisture content, and grain size were selected for evaluation of the AQUASAND model. The beaches selected for model verification along with their mineralogical and physical parameters used as inputed into AQUASAND are given in Table 1. Figure 4 shows the seven AQUASAND generated reflectance curves (in the .4-2.5 μm region of the spectrum) for the respective beaches. Superimposed on each of the seven curves appears the actual spectrum of the beach as measured using the ERIM Cary 14 spectroreflectometer.

These results are very encouraging, for although the absolute values of the curves differ, the overall shape and absorption bands seem to correspond remarkably well.

4.0 SUMMARY

The AQUASAND reflectance model has been satisfactorily evaluated. The model is currently being used to generate hypothetical sands, so that grain size and moisture prediction algorithms can be generated using remote sensed data.

A beach resembling the mineralogy of beach sample AD2 (see Table 1, and Figure 4) has been parametrically run with various moisture and grain sizes using AQUASAND. The generated spectral graphs similar to those shown in Figure 4 were then examined to determine optimum single or ratio spectral intervals to predict moisture and grain size.

A summary of that analysis is shown in Figure 5. The graph on the left of the figure shows ratio channels selected while the graphs on the right show single channels selected from AQUASAND parametrically varied results.

Currently AQUASAND is being used to generate beach sands where only one physical or chemical property is parametrically varied. Regression analysis is then applied to the AQUASAND results to obtain the finalized moisture and grain size prediction algorithms.

REFERENCES

G.H. Suits, The Calculation of the Directional Reflectance of a Vegetation Canopy, Remote Sensing of the Environment, Vol. 2, pp. 117-125, 1972.

Vincient, R.K. and G.R. Hunt, Infrared Reflectance from Material Surfaces, Applied Optics, Vol. 7, No. 1, 1958, pp. 53-59.

Vincient, R.K. and F.J. Thomson, Spectral Compositional Imaging of Silicate Rocks, J. Geophysical Res., 1972, pp. 2465-72.

Layer 1 is shown as consisting of grains of only one kind of mineral.
Layer 2 is shown to consist of a mixture of two kinds of minerals.
The equivalent Lambertian scattering panels are illustrated on the right.

FIGURE 1. CROSS SECTION OF SAND LAYERS

TABLE 1. BEACH SAND CONSTITUENTS

Sand	Mean Grain Sand
1. Carbonate 99% Carbonate 1% Organics	1 mm
2. D-Dune HI 95% Quartz 5% Feldspar	.19
3. MX2 98% Quartz 2% Carbonate	.22
4. BA1 98% Quartz 2% Feldspar	.40
5. EA2 90% Quartz 6% Feldspar 2% Kaolinite 2% Opaques	.28
6. AD2 98% Quartz 2% Feldspar	.38
7. HA1 55% Quartz 28% Feldspar 4% Kaolinite 13% Opaques	.32

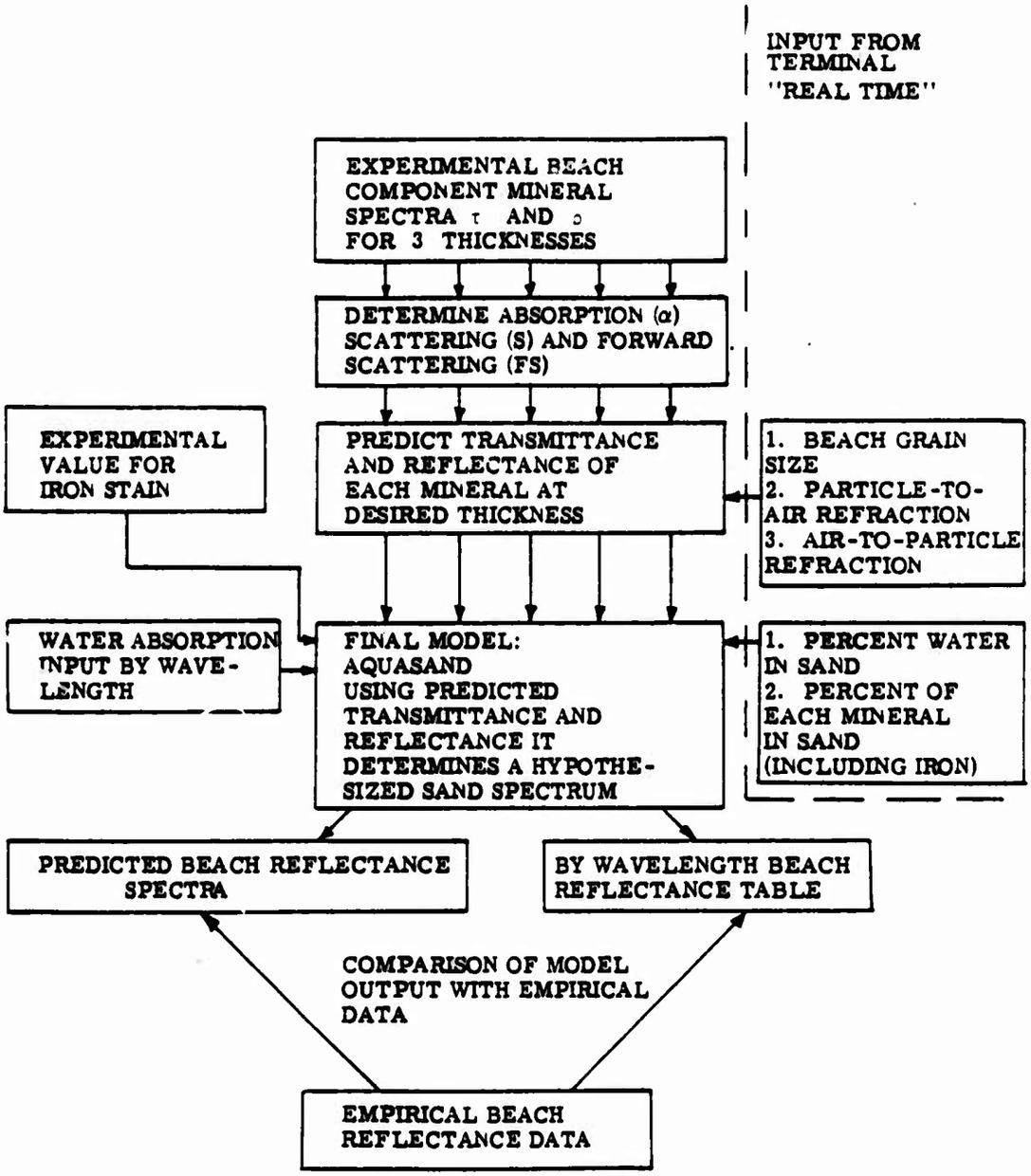

FIGURE 2. DIAGRAM OF MODEL FLOW

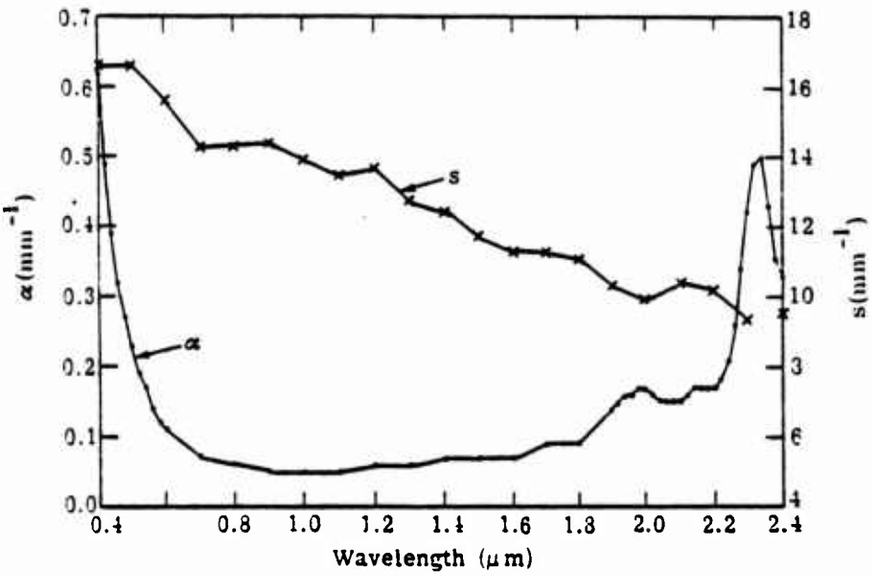

FIGURE 3. PLOT OF ABSORPTION (α) AND SCATTERING (s) FOR CARBONATE IN THE .4 TO 2.4 um REGION

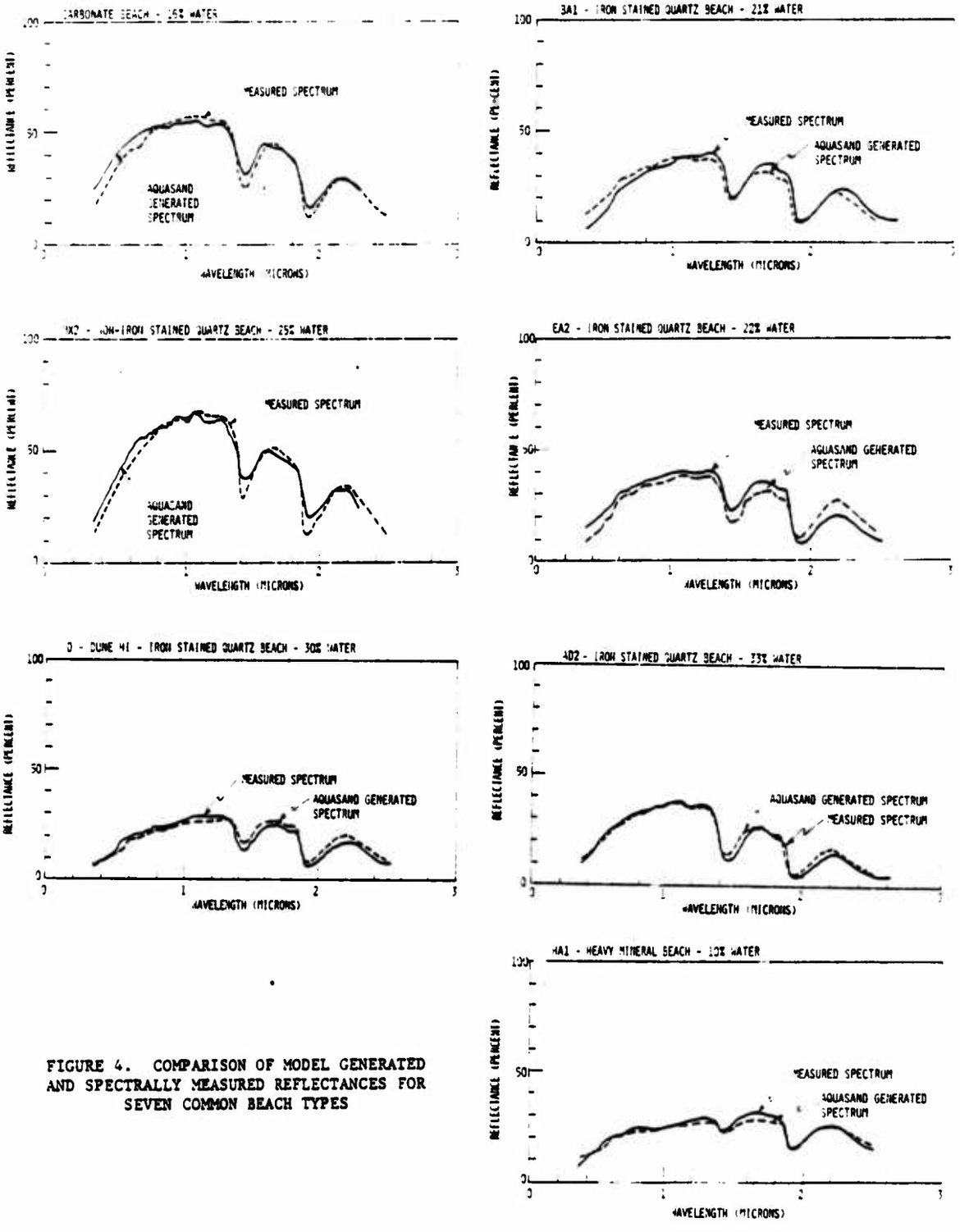

FIGURE 4. COMPARISON OF MODEL GENERATED AND SPECTRALLY MEASURED REFLECTANCES FOR SEVEN COMMON BEACH TYPES

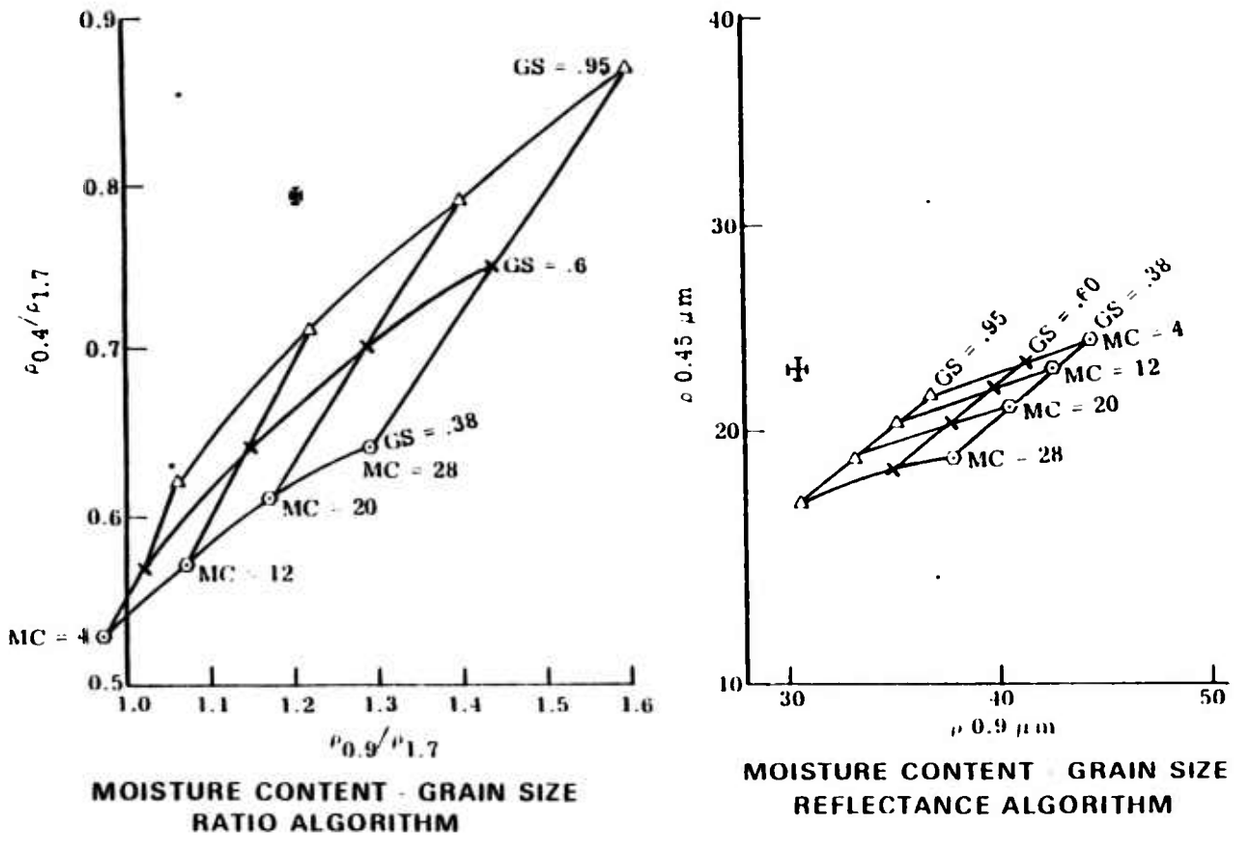

FIGURE 5. SINGLE BAND (RIGHT) AND RATIO REFLECTANCE ALGORITHMS FOR SEPARATING MOISTURE AND GRAINSIZE

EVALUATION OF HIGH RESOLUTION SIDE LOOKING AIRBORNE RADAR ON THE UNIVERSITY OF GUELPH TEST STRIP

Brian Brisco and Richard Protz
Department of Land Resource Science
University of Guelph
Guelph, Ontario. N1G 2W1

ABSTRACT

Imagery obtained from the four channel ERIM radar system was evaluated for soil survey and field type identification purposes. The area imaged was snow covered to a maximum depth of approximately 1 meter. An icy snow surface, high moisture content, or ice layers within the snowpack may have been the cause of attenuation of the X-HH signal, creating a lack of tonal variations. The other three channels exhibited tonality patterns which varied between and within channels and agricultural fields. These tonality patterns were not related to geologic or topographic influences, but low correlations with the soils map of the area were observed. Vegetation at these locations appeared to be the cause of these correlations. Grey scale values of the seven dominant field types encountered in the study area indicated that discrimination is possible using tonal signatures from all four channels of this SAR system. The cross-comparison of each channel's response value may separate fields with very similar averaged reflectance values. More ground truth and more effective use of ancillary data are needed to improve the interpretation procedure. A more quantitative method of the tonal measurement is also needed and combined with a measure of texture would greatly enhance the discriminative ability of radar systems. The combination of these improvements would make possible the digital classification of SAR data by computer. Thus multi-temporal and multi-spectral radar imagery, in combination with the effective use of ancillary data, have the potential to discriminate crops and soils for agricultural purposes.

RESUME

Des images de terrain enneigé, obtenues avec un système radar de quatre bandes, ont été évaluées en vues d'utilisation pour l'inventaire des sols ainsi que pour la reconnaissance des caractéristiques des surfaces agricoles. Une surface glacée, une teneur en eau élevée, ou des couches de glace à l'intérieur de la neige ont pu causer l'atténuation du signal X-HH créant ainsi un manque de variations dans la tonalité. Dans les trois autres canaux les tonalités des couleurs variaient entre les bandes et suivant le type de champs agricole. La tonalité des couleurs n'apparait pas être fonction de facteurs géolcgiques ou topographiques et les corrélations avec le relevé des sols pour la région sont pauvres. Ceci pourrait être dû aux influences du couvert végétal. Les valeurs obtenues dans l'échelle des gris pour les sept types de champs indiquent qu'une distinction est possible suivant les caractéristiques tonales de chacune des quatres bandes. En comparant les valeurs obtenues pour chaque bande, des champs avec dec réflectances "moyennes" très semblable peuvent être séparés . Ce procédé de discrimination pourrait être amélioré par une mesure plus quantitative du ton et une meilleure reconnaissance sur le terrain. Ce procédé pourrait amener une classification automatique par ordinateur des données obtenues avec un système SAR. Une telle imagerie au radar multi-temporelle et multi-spectrale, utilisée effectivement avec des données auxiliaires peut permettre d'identifier les récoltes et les sols agricoles.

INTRODUCTION

Tonal variations observed on radar images of the earth's surface depict the ability of the ground targets to reflect electromagnetic radiation incident on the imaged targets. The proportion of incident radiation returned to the radar sensor, i.e., backscatter, depends on dielectrical and geometrical properties of the ground elements. Various research efforts in the past have attributed the tone differences observed on radar imagery to characteristics of snow cover (Waite and MacDonald, 1970; Vickers and Rose, 1972), surface soil conditions (Morain and Campbell, 1974; Cihlar et al., 1975), and crop type (Haralick et al., 1970; Bush and Ulaby, 1975). Radar is a sensor of great potential to many kinds of studies in agronomy, but more research is needed on the interactions of the earth's surface and the radar waves to develop effective interpretation procedures.

With the advent of synthetic aperture radar systems (SAR), finer resolution imagery has provided more detailed representations of the earth's surface. Dual polarization, multi-frequency radar systems are the microwave equivalents of multispectral scanners, which have proven useful for many remote sensing applications (Haralick et al., 1970). The purpose of this study was to evaluate four channel SAR imagery, of snow covered terrain, for information pertaining to soil survey and cover type discrimination.

Presented to the 5th Canadian Symposium on Remote Sensing, Victoria, August 1978.

THE USE OF REMOTE SENSING IN THE DETERMINATION OF BEACH SAND PARAMETERS*

C.F. Davis, R.A. Shuchman, and G.H. Suits

Environmental Research Institute of Michigan
Ann Arbor, Michigan

ABSTRACT

A reflectance model (AQUASAND) was developed to gain insight into the spectral effects of changing mineralogy, moisture, and grain size related to beach sands. The model, a modification of the Suits radiative transfer vegetation canopy model, uses the transmittance and reflectance of the component minerals, the desired sand moisture content, and the desired sand grain size to produce a reflectance spectrum in the .35 to 2.5 μm range.

Using information from AQUASAND, a mineralogy, moisture, and grain size predictive algorithm (MOGS) was developed based on laboratory sand reflectance spectra. Input to the algorithm is a set of 17 spectral reflectance "bands" simulating an airborne multispectral scanner (MSS) configuration. The MOGS algorithm first determines the appropriate mineralogical class for the input sand. Within a given class, regression equations are used to determine moisture and grain size.

The predictive results of the MOGS algorithm are very encouraging. When tested on 70 of the sand reflectance spectra from which it was derived, the correlation of actual to predicted moisture was 96%. The correlation of actual to predicted grain size based on 46 samples was 88%. Tests on independently collected sand spectra yielded similar results. The algorithm was also successfully applied to actual MSS data, collected over the Lake Michigan coastline, to generate moisture distribution and grain size distribution digital images of the beach region.

1. INTRODUCTION

Historically remote sensing has been proven useful in the delineation of rock types most often with the applications of future mineral exploration in mind. In this investigation, beach sands were analyzed with the intention of determining not only mineralogy but also moisture and grain size. These three parameters are of interest from a beach trafficability and sediment transport point of view. Recognition of these parameters would also allow the identification of beach mineral deposits based on grain size and mineralogy. Since beaches are formed by intense erosion of the parent materials, harder minerals tend to be preserved and concentrated while others are dissipated. Depending on the origin of the sand, these residual minerals may be economically valuable.

In order to fully understand the effects of changes in mineralogy, moisture, and grain size on the spectral reflectance of beach sand, a sand reflectance model was used. The model, an adaptation of the Suits radiative transfer vegetation canopy model, is known as AQUASAND (Suits, 1972). It uses, as inputs,

*This work is supported by the Office of Naval Research (ONR) Contract No. N0014-74-C-0273. Mr. Hans Dolezalek is the ONR technical monitor.

the reflectance and transmittance for each mineral comprising the beach sand (i.e., quartz, feldspar, kaolinite, etc.). In addition, input to the model includes the sand grain size, the void space in the sand, and the moisture profile as a function of depth. By varying these input parameters insight was gained into the effect of physical changes on the bulk sand reflectance.

Using the information obtained from AQUASAND, the mineralogy, moisture, and grain size (MOGS) algorithm was developed using reflectance spectra measured on a Cary 14 spectrophotometer.* These spectra ranged from 0.35 to 2.5 μm, an interval practical for existing remote sensing technology. The MOGS algorithm was evaluated both on the reflectance spectra from which it was derived and on spectra collected following the algorithm development. In addition digital images of grain size distribution and moisture distribution were developed from actual multispectral scanner data.

2. PROCEDURE

The research involved in the construction of the MOGS algorithm was divided into two parts. First the Suits radiative transfer vegetation canopy model was converted to a model which could be applied to beach sands (AQUASAND) and, second, the MOGS algorithm was developed using insight obtained from the AQUASAND model.

2.1 THE AQUASAND MODEL

The most elementary model of sand reflectance is the simple plane mixture model. The model employs the assumptions that all sand particles are opaque and are randomly mixed. The surface of the sand is made up of the cross-sectional areas of the individual particles. The model calculates the bulk reflectance as being a weighted average of the particle reflectances. The model fails to achieve good accuracy because the transmittance of some particles in a finely divided state can be quite large and multiple scattering between particles is often significant.

A more complex model and the one used in this work, employs concepts identical to those employed in the directional reflectance model for vegetative canopies (Suits, 1972). Although a vegetative canopy and a sand profile are visually quite different, the essence of the reflection, transmission, and multiple scattering phenomena is much the same for both cases.

2.1.1 MODEL ASSUMPTIONS

The first assumption of the model is that the scattering components are distributed in more or less uniform layers. Because of the wind and wave action involved in the creation of a beach, sand profiles tend to be vertically stratified into horizontal layers and thus the assumption is satisfied.

The second assumption of the model is that spectral flux interacting with the sand may be divided into two types: specular and diffuse. Specular flux represents radiation which passes between the sand grains through voids and cracks without deviation. All incoming radiation is specular before it reaches the sand surface. Diffuse flux is some fraction of the specular flux which has been intercepted by a scattering component (sand grain) at least once. Following this interception it may be scattered forward or backwards, either interacting with other sand particles, or heading upwards to the sensor.

A third assumption of the model is that the individual particles making up the sand can be represented by a set of horizontal and vertical Lambertian panels which have the same reflectance and transmittance properties as do the sand particles. This assumption defines a simplified scattering phase function which allows the calculation of ensemble reflectances in closed form. Fortunately

*(The Cary 14 spectrophotometer is a device which is capable of digitally recording the reflectance spectrum of a surface in the .35 to 2.5 μm range.)

in sands, as in vegetative canopies, multiple scattering dominates over phase function scattering because of the high density of the scattering components. This characteristic greatly simplifies the necessary model calculations.

The fourth assumption of the model is that the diffuse flux moves in a Lambertian manner, both upward and downward, as a first approximation. The ensemble reflectance need not be perfectly Lambertian, however, it should be approximately so. Both vegetation and sand meet this criterion.

As mentioned earlier the AQUASAND model operates on the reflectance (ρ) and transmittance (τ) of a set component minerals for a given grain size to predict the reflectance spectrum of a beach. One method of obtaining the necessary ρ and τ values would be to measure them exactly for each potential grain size. This would potentially require many measurements and considerable sample preparation. Another method, and the one used in this study would be to derive the components of transmittance and reflectance for each mineral and analytically predict the ρ and τ for any given grain size. The necessary components needed to derive such information are absorption (a), internal scattering (s), and the forward scattering fraction (FS). These basic measurements were obtained by measuring the τ and ρ of 3 thin sections of each potential mineral type. Each thin section was a slightly different thickness than the others. By using an iterative curve fitting procedure the a, s, and FS values were derived using the Duntley equations (Duntley, 1942). With these values calculated at 10 nm interval throughout the spectrum we were able to predict the transmittance and reflectance spectra of a given mineral and any grain size we chose. The ρ and τ values were then entered into the AQUASAND model to produce a bulk sand reflectance spectrum (Figure 1).

Moisture content was entered into the model by adding an appropriate water spectral absorption factor at each wavelength for which a spectral value was computed for the sand. By entering the desired percent-by-volume water content the correct attenuation due to water was computed within the optical pathway equations.

2.1.2. MODEL RESULTS AND EVALUATION

By manipulating the mineralogical, grain size, and moisture model input parameters we were able to "create" any sand type we wished. Model generated spectra were compared to empirical spectra obtained from seven diverse beach types (Figure 2). The empirical measurements were made on a Cary 14 spectrophotometer which allows both continuous scanning of spectra in the .35 to 2.5 μm range and digital recording of the output spectra.

The carbonate beach type (Figure 2a) is composed of 99% exoskelatal fragments of marine organisms with approximately 1% dark organic debris mixed in. Carbonate sands are characteristically high in reflectance with high reflectance in the "red" spectral region (0.6 μm). As is apparent in Figure 2 the model captures this characteristic quite well.

Figure 2b and c are spectra of predominately iron-stained quartz beaches characteristic of the Delaware coastline. In general these spectra are depressed due to the iron staining and have substantial amounts of feldspar incorporated with them.

Figure 2d is a non-iron stained, 98% pure quartz beach. This beach type is typical of that found on the Gulf of Mexico coastline. These beaches have high reflectance due to the lack of iron stain and other dark minerals. Besides quartz there are trace amounts of carbonate and organic matter amounting to approximately 2%.

Figure 2e and f are spectra of iron-stained beaches from the Lake Michigan coastline. Both sands exhibit relatively low reflectance although spectrum 2f is definitely the lower of the two. This difference is related to the more intense iron-staining and larger percentage of opaque rock fragments in the latter beach type.

Figure 2g is a heavy mineral beach spectra collected on the coast of Oregon, which exhibits a characteristically low reflectance in the visible region. This is due to a high amount of iron-staining in addition to a large percentage of high density, opaque minerals (i.e., ilmenite, magnetite, etc.). Beaches of this type tend to have relatively low percentages of quartz, on the order of 30 to 40 percent, coupled with equal amounts of feldspar. Except for minor errors, the AQUASAND model correctly predicted the spectrum of the empirically measured sand in all seven cases. With this successful validation, work began on the algorithm predicting mineralogy, moisture, and grain size based on sand reflectance spectra in the .33 to 2.5 μm range.

2.2 DEVELOPMENT OF THE MOGS ALGORITHM

From inspection of both the AQUASAND generated, and empirical spectra it became apparent that mineralogy had by far the greatest influence on bulk reflectance. So great is this influence that it tends to mask the more subtle features of changes in grain size and, to a much lesser extent, moisture. It was decided that in order for the algorithm to handle a broad variety of sand types and still maintain the resolution needed to detect small spectral features, a preprocessing classification of mineralogy would be necessary.

2.2.1 THE CLASSIFICATION OF MINERALOGY

In order to discriminate mineralogy a vector length decision framework was used. The concept is developed as follows.

Suppose that there are two points, A and B, located in two dimensional space. The distance, or vector length, L, from A and B can be expressed in terms of the X and Y coordinate locations of points A and B as:

$$L = \sqrt{(X_A - X_B)^2 + (Y_A - Y_B)^2} . \qquad (1)$$

This is, of course, related to the Pythagorean Theorem. Now suppose we have a p-dimensional system with A and B located in each dimension. The vector length can be expressed as

$$L = \sqrt{\sum_{i=1}^{p} (X_{iA} - X_{iB})^2} , \qquad (2)$$

where X_{iA} is the location of point A in the ith dimension and X_{iB} is the location of point B in the ith dimension.

This rationale can be used to classify some point, T, as being the member of one of n classes (A_j, j=1,n), by finding the minimum vector length from T to A_j(j=1,n). In other words T is said to be a member of the class which is closest to it, on the average, across all p dimensions. The minimum vector length is defined as

$$L_{min} = \min_{j=1,\ldots,n} \sqrt{\sum_{i=1}^{p} (X_{iT} - X_{iAj})^2} . \qquad (3)$$

Notice that equation 3 has no provision for variability in the n classes, therefore, L_{min} is chosen as being the shortest linear vector length. If each class has the same variability associated with it this causes no difficulty. In this experiment, however, there were considerable differences in variability between the classes so that a modification of equation 3 had to be made. The standard deviation (SD) was used to modify the distance between T and Aj related to each dimension thus removing the effects of variability from each class. This normalized minimum distance equation is expressed as

$$L_{min} = \min_{j=1,\ldots,n} \sqrt{\sum_{i=1}^{p} (X_{iT} - X_{iAj})/SD_{ij}^2} , \qquad (4)$$

where SD_{ij} is the standard deviation associated with the j^{th} class in the ith dimension.

In the application of this method to the classification of mineralogy, the "dimensions" are spectral bands or ratios of spectral bands and the "classes" are mineralogical types. Eight spectral bands (Table 1) and all possible unique ratios of those spectral bands were used to classify the mineralogical type of an input sand as one of five categories (Table 2). The object was to make each category as homogeneous as possible so that the moisture and grain size regressions which followed would be sensitive to small scale spectral changes.

2.2.2. THE DEVELOPMENT OF MOISTURE AND GRAIN SIZE REGRESSIONS

Using the AQUASAND model we found that information related to moisture content of sands is best derived from the spectral region beyond 1.0 μm. This is due to the fact that the spectral reflectance of sand in this region is reduced by absorption in proportion to the amount of water present. Exceptionally high spectral absorption is noted near 1.4 and 1.9 μm. Although the spectral reflectance in these regions is highly correlated to moisture we did not consider them since atmsopheric absorption prohibits their use by an airborne sensor.

Changes in grain size seem to manifest themselves most clearly in the shorter wavelengths (.4-.7 μm). Grain size information is gained by light being reflected from sand grains below the surface through surface grains. The transmittance through the surface grains is reduced by internal scattering and absorption of the particle. Since both of these factors are dependent on thickness, the bulk reflectance of a sand is dependent to some degree on the grain size. Theoretically a large grain sand should have a lower reflectance than a small grain sand of the same mineralogical composition and with similar moisture content. According to our measurements this appears to be the case.

This grain size phenomenon can be confounded in two ways. First if there is no scattering or absorption within the grains (i.e., a perfectly clear material at all wavelengths) there can be no attenuation. Fortunately, even in our purest quartz sands there were enough impurities and inclusions to give some attenuation. Second, the sand grains may be opaque and thus attenuate too much light. This appears to be the case in the heavy mineral and carbonate beaches. Most of the bulk reflectance for these two types was due to surface reflectance and little if any was due to light transmitted through the surface grains from below. We were unable to create accurate grain size equations for these types.

Utilizing the physical phenomena discussed above we were able to develop multiple linear regression equations for predicting moisture in all five mineralogical classes and grain size for three of the five mineralogical classes. The basis for all the regressions except one was the sample group corresponding to a given mineralogical class. The single exception was the grain size equation corresponding to a pure quartz beach. Our samples within this type consisted of a single grain size (0.22 mm) and, as such did not provide an adequate basis for regression equations. For this case we used AQUASAND generated spectra to simulate a wide range of grain sizes in order to add grain size variability to the data set.

Seventeen spectral bands between 0.4 and 2.5 μm were chosen for use in the regressions (Table 3). Within the 17 bands, only those which were predicted by the AQUASAND model to be most informative were used. In this way we could be reasonably certain that the regression equations would respond the correct parameter and thus yield accurate predictions. The predictive equations together with the associated standard errors (SE), and coefficient of variation (R^2) are given in Table 4.

In summary the MOGS algorithm (Figure 3) represents a computer controlled package of equations. The input is a set of 17 spectral reflectance bands obtained from an unknown sand. Based on these bands, the sand is classified as being a member one of five mineralogical types. Depending on the mineralogical type, the appropriate moisture and grain size (where applicable) equations are applied to the data. The output from the MOGS algorithm is the predicted mineralogical class, the predicted moisture, and the predicted grain size.

3. TEST RESULTS OF THE MOGS ALGORITHM ON LABORATORY SPECTRA

The MOGS algorithm was first tested on 70 of the 81 samples from which it was derived and the results were very promising as can be seen in Table 5. The classification of mineralogy was 99+% correct. The overall correlation of predicted to actual moisture was 96% (significant at the .001 level) and the overall correlation of predicted to actual grain size was 88% (significant at the .001 level). However, testing any equation or algorithm on the samples from which it was derived is not conclusive. For this reason the MOGS algorithm was tested on several other beach sand samples which were independently collected and spectrally measured following the algorithm construction. These results are given in Table 6. In each case the MOGS algorithm selected a mineralogy which allowed the moisture and grain size regression to operate correctly. The independent test yielded an actual moisture to predicted moisture correlation of .95 (significant at the .01 level). The prediction of grain size was in no case more than 0.07 mm different from the actual grain size.

4. TEST OF THE MOGS ALGORITHMS ON MSS DATA

The next logical test for the MOGS algorithm was to evaluate it on actual MSS data. Such an investigation is presently underway using data obtained from the Environmental Research Institute of Michigan (ERIM) multispectral-scanner (MSS) flown over a portion of the Lake Michigan shoreline (November 1, 1978). The MOGS algorithm was modified to conform to the 12 band configuration of the ERIM scanner.

Although a complete discussion of the Lake Michigan MSS test is beyond the scope of this paper, preliminary results look quite good (Table 7). The correlation of predicted to actual moisture content is .91 (significant at the .01 level) and the prediction of grain size is, in no case, greater than .09 mm different from the actual grain size.

The moisture prediction appears particularly poor for high moisture contents. This may be due to the fact that wet sand at the test sites appeared to exhibit bi-directional dependencies (i.e., a failure to behave in a Lambertian manner). These bi-directional characteristics are enhanced at low sun angles and are not accounted for by the MOGS algorithm. Although the flight took place at 1:30 EST the sun was only 38° above the horizon on November 1. To minimize bi-directional reflectance, future aircraft flights should be made during complete mid-altitude (3000 m) cloud cover or sunny skies with the sun close to the zenith (summer sun).

Applying the same moisture and grain size equations used in the previous analysis, the entire Pentwater State Park beach on a pixel by pixel basis (in this case 1.5 x 1.5 meters) was classified with respect to grain size and moisture content. The two MOGS generated digital maps (see Figure 4) show the predicted moisture and grain size distributions on the beach at Pentwater. The ground truth measurements taken at the time of flight correlate well with these images. Figure 4 helps to demonstrate how an entire sandy coastline could be analyzed in respect to moisture, grain size, and gross mineralogy using a small subsection as calibration.

5. CONCLUSION

The development of the MOGS algorithm has demonstrated the feasibility of obtaining quantitative moisture and grain size information from the spectral reflectance of beach sands. The determination of grain size is dependent on the sand grains being neither opaque or perfectly clear.

The two stage nature of the MOGS algorithm is directly responsible for its broad applicability without loss of detail. By separating the mineralogical types prior to the prediction of moisture and grain size much of the variability which could easily hide small scale changes is removed. The use of a vector length discriminant function to classify mineralogy worked extremely well in this application, since 36 different dimensions could be simultaneously evaluated. The use of a multistage approach involving multiple classification

techniques is a powerful tool; one which will very likely be useful in many areas of remote sensing.

The Lake Michigan field test has further demonstrated the MOGS algorithm's applicability to actual remotely sensed data. Grain size was predicted to within .09 mean diameter of actual while beach moistures less than 20% were accurately predicted. In all cases the computer algorithm correctly identified the Michigan beach mineralogy as being a predominantly quartz iron stained-feldspar beach.

Table 1. The 8 spectral bands used in the breakdown of beach mineralogy into 1 of 5 categories. In addition to these 8 bands all unique ratio combinations were also used.

Band #	Wavelength Range (μm)
1	.43-.47
2	.47-.49
3	.51-.53
4	.53-.56
5	.59-.63
6	.80-.90
7	.90-1.0
8	1.0-1.1

Table 2. The 5 potential mineralogical classifications

Class #	Description
1	Iron stained Atlantic coast type
2	Iron stained Michigan coast type
3	Iron stained pure quartz type
4	Heavy mineral type
5	Carbonate type

Table 3. The 17 bands used in the development of moisture and grain size regression equations

Band #	Wavelength Range (μm)
1	0.43-0.47
2	0.47-0.49
3	0.49-0.51
4	0.51-0.53
5	0.53-0.56
6	0.56-0.59
7	0.59-0.63
8	0.63-0.67
9	0.70-0.75
10	0.75-0.80
11	0.80-0.90
12	0.90-1.00
13	1.00-1.10
14	1.10-1.20
15	1.20-1.35
16	1.50-1.85
17	2.10-2.50

Table 4. Multiple linear regression equations for the prediction of moisture and grain size. The equations are listed by mineralogical class. Grain size is in mm.

a. Iron stained quartz - Atlantic coast

Predicted moisture % = $67.964 - 65.046 \left(\frac{\text{Band 16}}{\text{Band 14}}\right)$

S.E. = 3.08%, $R^2 = 0.888$

Predicted grain size = $6.87 - 3.4634 \text{ (Band 7)}^{1/4} + .0300 \text{ (Band 1)} + .01672 \text{(Band 15)}$

S.E. = 0.13 mm, $R^2 = 0.603$

b. Iron stained quartz - Michigan coast

Predicted moisture % = $60.149 - 49.961 \left(\frac{\text{Band 16}}{\text{Band 11}}\right) - 2.226 \left(\frac{\text{Band 17}}{\text{Band 1}}\right)$

S.E. = 2.56%, $R^2 = .970$

Predicted grain size = $0.6405 - 0.0152 \text{ (Band 5)} - .0047 \text{ (Band 17)}$

S.E. = 0.055 m, $R^2 = 0.558$

c. Non-Iron stained quartz

Predicted Moisture % = $127.02 - 65.159 \left(\frac{\text{Band 16}}{\text{Band 15}}\right) - 64.054 \left(\frac{\text{Band 15}}{\text{Band 14}}\right)$

S.E. = 2.12%, $R^2 = 0.971$

Predicted grain size = $1.158 - 2.328 \text{ (Band 10)} + .3201 \left(\frac{\text{Band 7}}{\text{Band 1}}\right) + 0.2858 \text{ (Band 16}$

S E. and R^2 not applicable

d. Carbonate

Predicted moisture % = $596.28 - 642 \left(\frac{\text{Band 14}}{\text{Band 17}}\right) - 1.081 \text{ (Band 14)} + 0.1538 \text{ (Band 17)}$

S.E. = 4.09%, $R^2 = .879$ No grain size equation.

e. Heavy mineral

Predicted Moisture % = $19.284 + 11.194 \left(\frac{\text{Band 14}}{\text{Band 17}}\right) - 1.081 \text{ (Band 14)} + 0.1538 \text{ (Band 17)}$

S.E. = 4.09%, $R^2 = .879$ No grain size equation.

Table 5. Comparison of actual sand parameters to predicted classification by the MOGS algorithm

Sand I.D.		Moisture %		Grain Size mn	
Actual	Predicted	Actual	Predicted	Actual	Predicted
A1	A	4.5	3.8	.35	.36
A2	A	29.4	26.4	.35	.46
A3	A	15.0	11.8	.37	.40
A4	A	28.4	28.0	.50	.48
A5	A	11.3	12.9	.43	.49
A6	A	33.4	27.1	.32	.39
A7	A	13.1	13.8	.35	.43
A8	A	24.9	27.3	.38	.37
A9	A	8.8	19.4	.44	.30
A10	A	29.7	27.9	.43	.44
B1	B	21.0	17.8	.40	.62
B2	B	24.6	25.5	.76	.58
B3	B	14.2	15.1	.46	.57
B4	B	27.2	26.3	.88	.76
B5	B	11.0	8.9	.63	.82
B6	B	19.0	25.6	.95	.76
B7	B	26.8	28.2	.71	.76
B8	B	24.9	21.0	.76	.63
B9	B	6.2	5.9	.71	.62
B10	B	*	7.5	.71	.57
B11	B	20.0	23.0	.81	.76
B12	B	34.0	33.1	.69	.73
B13	A	6.0	4.4	.55	.60
B14	B	31.0	26.0	.83	.71
B15	B	18.0	22.2	.67	.69
B16	B	32.0	31.5	.57	.72
B17	B	18.0	20.8	.56	.67
B18	B	23.0	23.9	.65	.76
B19	B	3.0	7.1	.94	.68
B20	B	23.0	27.8	.60	.61
M1	M	5	8.2	.36	.27
M2	M	15	13.4	.36	.28
M3	M	25	26.2	.36	.34
M4	M	30	27.4	.36	.36
M5	M	5	5.5	.41	.38
M6	M	15	15.7	.41	.45
M7	M	0	0.0	.23	.31
M8	M	0	0.0	.29	.29
M9	M	0	0.0	.41	.39
M10	M	0	0.0	.36	.35
M11	M	10	12.0	.23	.31
M12	M	25	24.4	.23	.28
M13	M	30	27.2	.23	.25
M14	M	10	12.8	.41	.36
M15	M	20	20.6	.41	.40
M16	M	15	16.8	.23	.26
01	H	0	0	no grain size	
02	H	5	6.4	no grain size	
03	H	10	11.7	no grain size	
04	H	15	20.3	no grain size	
05	H	20	22.0	no grain size	
06	H	25	21.9	no grain size	
07	H	30	27.5	no grain size	

*No moisture data

Table 5. (Continued)

Sand I.D.		Moisture %		Grain Size mn	
Actual	Predicted	Actual	Predicted	Actual	Predicted
08	H	35	24.7	no grain size	
MX1	MX	25	24.6	.22	.32
MX2	MX	0	0.0	.22	.10
MX3	MX	10	14.1	.22	.13
MX4	MX	15	18.1	.22	.22
MX5	MX	30	34.2	.22	.4
MX6	MX	35	33.7	.22	.34
MX7	MX	20	23.1	.22	.33
MX8	MX	5	6.9	.22	.11
C1	C	0	0	no grain size	
C2	C	10	7.8	no grain size	
C3	C	5	5.7	no grain size	
C4	C	20	13.4	no grain size	
C5	C	15	18.8	no grain size	
C6	C	30	30.8	no grain size	
C7	C	25	27.9	no grain size	
C8	C	40	38.4	no grain size	
C9	C	50	46.4	no grain size	

Table 6. Comparison of actual parameters to predicted classificattions by the MOGS algorithm. Samples used here were collected independently of those on which the algorithm is based.

Sample Mineralogy		Moisture %		Grain Size (mm)	
Actual	Predicted	Actual	Predicted	Actual	Predicted
MICH1	MICH	37.7	25.6	.26	.28
MICH2	MICH	3.2	3.7	.28	.30
MICH3	MICH	0.3	0.0	.25	.32
MICH4	MICH	12.1	16.0	.23	.29
MICH5	MICH	15.0	12.7	.25	.30
MICH6	MICH	28.0	26.2	.28	.29

Table 7. Comparison of actual parameters to predicted classifications by the MOGS algorithm. The sand spectra used here were collected by the ERIM MSS.

Sample Mineralogy		Moisture %		Grain Size (mm)	
Actual	Predicted	Actual	Predicted	Actual	Predicted
MICH1	MICH	22.3	12.1	.25	.32
MICH2	MICH	1.0	0.0	.23	.28
MICH3	MICH	8.0	10.1	.22	.25
MICH4	MICH	28.0	16.9	.26	.35
MICH5	MICH	5.0	2.2	.24	.26

LITERATURE CITED

Duntley, S.Q. 1942. The Optical Properties of Diffusing Materials, Journ. Amer. Opt. Soc. Vol. 32, p. 61-69.

Suits, G.H. 1972. The Calculation of the Directional Reflectance of a Vegetation Canopy. Rem. Sens. of Env. Vol. 2, pp. 117-125.

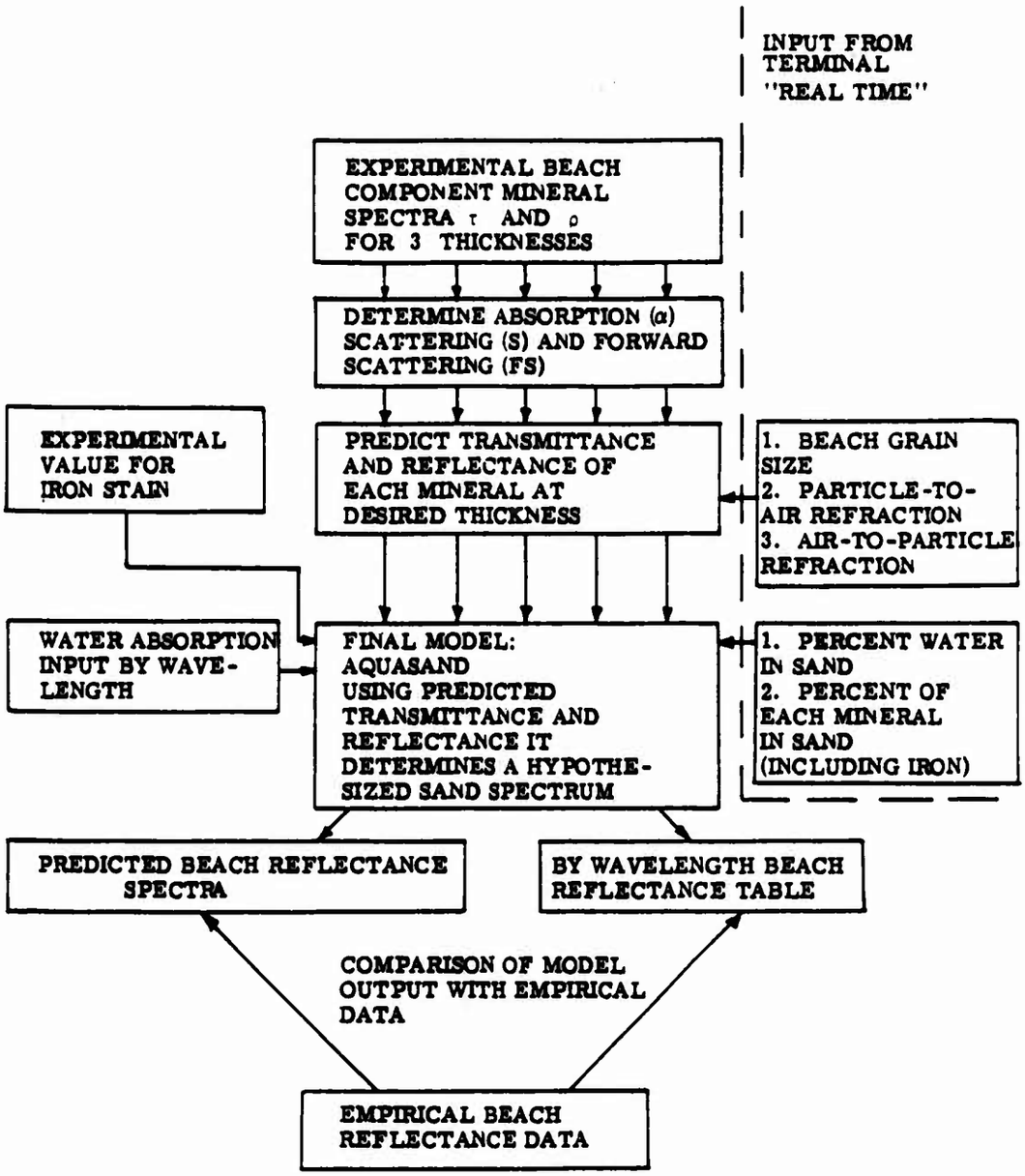

Figure 1. Flow diagram of the AQUASAND MODEL.

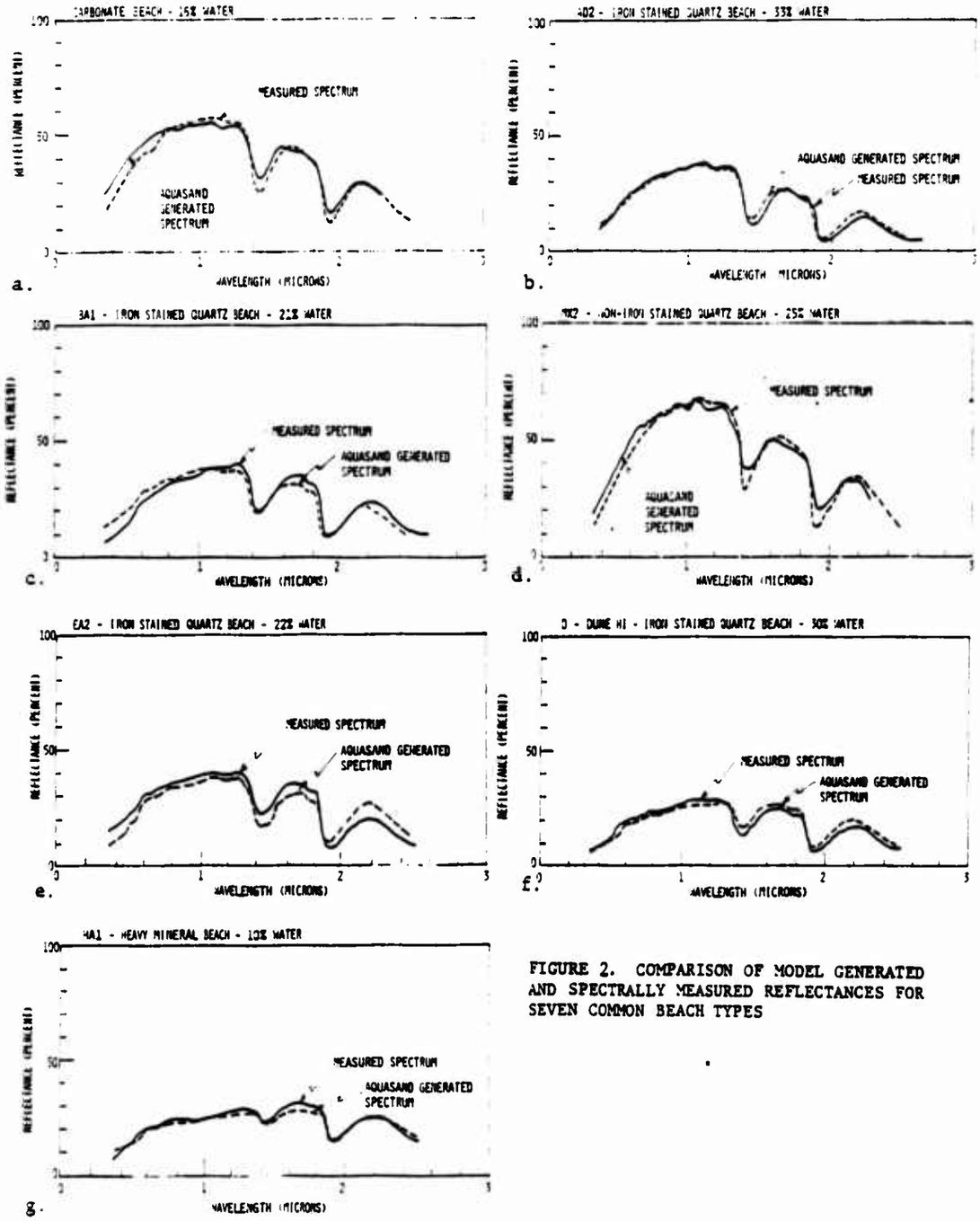

FIGURE 2. COMPARISON OF MODEL GENERATED AND SPECTRALLY MEASURED REFLECTANCES FOR SEVEN COMMON BEACH TYPES

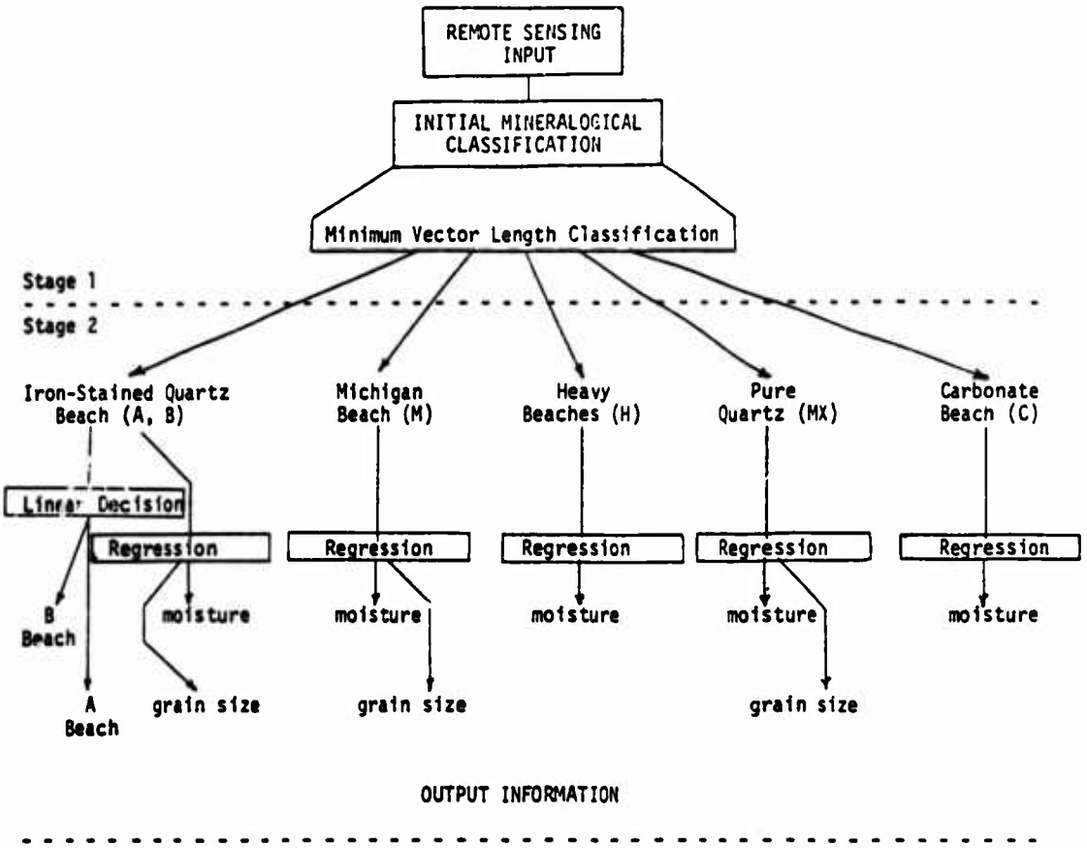

FIGURE 3. FLOW DIAGRAM OF THE MOGS ALGORITHM.

MOISTURE DISTRIBUTION IMAGE - LIGHTER SHADE INDICATES HIGHER MOISTURE CONTENT

0-5% 5-20% 20+%

GRAIN SIZE DISTRIBUTION IMAGE - LIGHTER SHADE INDICATES LARGER GRAIN SIZE

.15-.25 mm .25-.40 mm >.40 mm

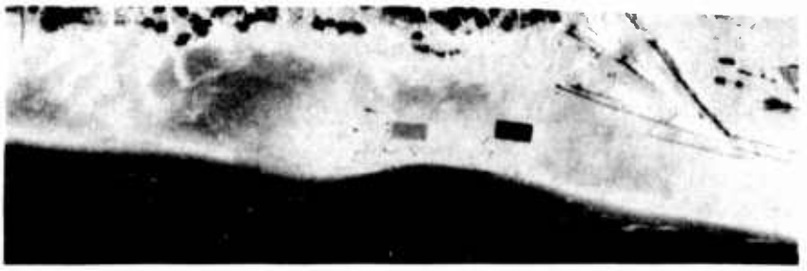

PANCHROMATIC AERIAL PHOTOGRAPH

FIGURE 4. DIGITAL IMAGERY, GENERATED BY THE MOGS ALGORITHM SHOWING THE DISTRIBUTION OF MOISTURE AND GRAIN SIZE ON PENTWATER BEACH (PENTWATER STATE PARK, MICHIGAN). WHITE AREAS ARE EITHER UNCLASSIFIED REGIONS OR OPEN WATER.

DETERMINATION OF BEACH SAND PARAMETERS USING REMOTELY SENSED AIRCRAFT REFLECTANCE DATA

Robert A. Shuchman

Environmental Research Institute of Michigan (ERIM)
P. O. Box 8618
Ann Arbor, Michigan 48107

and

David K. Rea

Department of Atmospheric and Oceanic Science
The University of Michigan
Ann Arbor, Michigan 48109

ABSTRACT

An algorithm was developed which determines the mineralogy, moisture, and grain size of beach sands based on the hemispherical reflectance in 17 discrete spectral bands. The bands chosen range between 0.40 and 2.5 μm, a wavelength range practical for existing multispectral remote sensing technology. The sand spectra on which the mineralogy, moisture, and grain size algorithm (MOGS) is based were obtained from laboratory spectrophotometric measurements. Selected spectral bands are used in a vector-length-decision framework to determine the mineralogical class of the input sand. Multiple linear regressions are then used, within a given mineralogical class, to determine the moisture and grain size of the sand.

The predictive results of the MOGS algorithm are very encouraging. When tested on 70 of the sand reflectance spectra from which it was derived, the correlation of actual to predicted moisture and grain size was 96% and 88%, respectively.

The MOGS algorithm has been successfully tested using aircraft multispectral scanner (MSS) data collected over the Lake Michigan shoreline. The algorithm correctly identified gross mineralogy and predicted grain size to within 0.09 mm of measured values. Some difficulties were encountered in predicting high beach sand moistures, probably due to the increasing non-Lambertian nature of sand as the moisture content of the sand increased.

INTRODUCTION

During the past ten years remote sensing has been proven capable of delineating outcrop lithologies, a procedure often carried out in the early stages of mineral exploration. Typically, remote-sensing spectral data are compared to those in a reference library containing laboratory-acquired spectral data of individual minerals and rocks. Through the use of a computer, correlations are made between the reference and remote-sensing spectra in an attempt to identify the surface material (Vincent, Thomson and Watson, 1972).

In this investigation, beach sands were analyzed with the intent of determining not only mineralogy but also moisture and grain size. These three parameters are of interest from both geological and engineering points of view. The mean grain size at a reference point on a beach is a fundamental characteristic of the beach. Studies have indicated that mean grain size is related to beach face slope (Komar, 1976), water percolation and permeability and ease of grain movement (Komar, 1977; Zenkovich, 1967; Huntley and Bowen, 1975; Fraser and Hester; 1977; Self, 1977). These factors play a major role in determining if a beach will be erosional or depositional under different wave conditions (Madsen and Grant, 1976; Swart, 1976).

Additionally, recognition of these three sand parameters would also allow the identification of beach mineral deposits based on grain size and mineralogy. Since beaches are formed by intense erosion of the parent materials, more resistant minerals tend to be preserved and concentrated while others are dissipated. Depending on the origin of the sand, these residual minerals may be of economic value.

In order to determine the mineralogy, moisture, and grain size of a given sand, a two-stage vector-length-decision and multiple linear regression approach was used. This entailed, first, the breakdown of mineralogy into five categories. Each category was then analyzed for moisture content and grain size using predictive multiple linear regressions based on selected spectral bands.

BACKGROUND

The theoretical basis for the work presented in this paper was developed over a period of approximately ten years. Studies have been made towards understanding the effects that grain size, moisture coating, and mineralogy of particulates have on reflected radiation from beach sands. It was shown by Emslie (1966) and Aronson, et al, (1967) that reflected radiation from beach sand is a function of: the wavelength of the radiation; the optical constants of the medium, i.e., n (refractive index) and k (index of absorption); the particulate grain size; the packing density; and the roughness of the surface. Vincent and Hunt (1968) used reflectance data based on ground laboratory samples to improve on the work of Aronson, et al. The model of Vincent and Hunt also accounted for volume scattering of reflected radiation in sand particles.

Leu (1977) working at the Environmental Research Institute of Michigan (ERIM) collected beach sands (from Delaware) and measured their reflectance in the laboratory in the 0.4 to 2.5 μm range using a Cary 14 laboratory spectrophotometer. (The Cary 14 spectrophotometer is a device which is capable of digitally recording the reflectance spectrum of a surface in the 0.35 to 2.5 μm range.) Leu then used multiple linear regression to correlate

reflectance values in discrete reflectance bands to moisture and grain size. Leu's work showed promise, but his regressions did not work when beach sand reflectance values other than those from Delaware beaches were used. This indicated the mineralogy of a beach sand strongly affects its reflectance spectra and that the effects of mineralogy must be understood before moisture and grain size prediction algorithms can be run.

In order to understand fully the effects of changes in mineralogy, moisture, and grain size on the spectral reflectance of beach sand, a sand reflectance model was used. The model, an adaptation of the Suits radiative transfer vegetation canopy model, is known as AQUASAND (Suits, 1972). It uses, as inputs, the reflectance and transmittance for each mineral comprising the beach sand (i.e., quartz, feldspar, magnetite, etc.). In addition, input to the model includes the sand grain size, the void space in the sand, and the moisture profile as a function of depth. By varying these input parameters insight was gained into the effect of physical changes on the bulk sand reflectance.

Using the information obtained from AQUASAND (Shuchman, et al., 1978) the mineralogy, moisture, and grain size (MOGS) algorithm was developed using reflectance spectra measured on a Cary 14 spectrophotometer. These spectra ranged from 0.35 to 2.5 μm, an interval practical for existing remote sensing technology. The MOGS algorithm was evaluated both on the reflectance spectra from which it was derived and on spectra collected following the algorithm development. In addition, digital images of grain size distribution were developed from actual multispectral scanner data.

DEVELOPMENT OF THE MOGS ALGORITHM

The procedure of developing an algorithm to predict mineralogy, moisture and grain size of beach sands was divided into three segments. First, a data base of sand reflectance values was selected from which to build the algorithm, second, the necessary equations were developed, and third, the algorithm was evaluated using actual remotely sensed aircraft data.

All of the equations that make up the mineralogy, moisture, and grain size (MOGS) algorithm are based ultimately on 81 laboratory measured reflectance spectra of beach samples obtained from a Cary 14 spectrophotometer operated by the Environmental Research Institute of Michigan (ERIM). The sand samples were collected from five diverse beach types located in various coastal areas of the continental United States between June 1974 and October 1978. The use of a large range of sand types was deemed necessary to give the MOGS algorithm a wide field of applicability. The mean grain size (diameter), moisture content, and approximate location of each beach sand sample used in the development of the MOGS algorithm are given in Table 1.

From inspection of both the AQUASAND generated, and empirical spectra it became apparent that mineralogy had by far the greatest influence on the reflectance spectra. So great is this influence that it tends to mask the more subtle features of changes in grain size and, to a much lesser extent, moisture.

In order to achieve the fine detail needed for the classification of moisture and grain size while still maintaining the applicability to a large range of mineralogies a two-stage procedure was established in the development of the MOGS algorithm (Figure 1). The first stage entails

TABLE 1

The mean grain sizes and moisture contents of the 81 sand samples used in the development of the MOGS algorithm. Samples are given by mineralogical class.

Sand I.D.	Moisture Content (%)	Mean Grain Size (mm)	Sand I.D.	Moisture Content (%)	Mean Grain Size (mm)
A1	4.5	.35	M12	25.0	.23
A2	29.4	.35	M13	30.0	.23
A3	15.0	.37	M14	10.0	.41
A4	28.4	.50	M15	20.0	.41
A5	11.3	.43	M16	15.0	.23
A6	33.4	.32	M17	22.0	.28
A7	13.1	.35	M18	2.0	.31
A8	24.9	.38	M19	8.0	.26
A9	8.8	.44	H1	0.0	.32
A10	29.7	.43	H2	5.0	.32
B1	21.0	.40	H3	10.0	.32
B2	24.6	.76	H4	15.0	.32
B3	14.2	.46	H5	20.0	.32
B4	27.2	.88	H6	25.0	.40
B5	11.7	.63	H7	30.0	.40
B6	19.0	.95	H8	35.0	.40
B7	6.8	.71	H9	0.0	.17
B8	24.9	.76	H10	15.0	.22
B9	6.2	.71	H11	10.0	.32
B10	21.3	.71	H12	5.0	.40
B11	20.0	.81	MX1	25.0	.22
B12	34.0	.69	MX2	0.0	.22
B13	6.0	.55	MX3	10.0	.22
B14	31.0	.83	MX4	15.0	.22
B15	18.0	.67	MX5	30.0	.22
B16	32.0	.57	MX6	35.0	.22
B17	13.0	.56	MX7	20.0	.22
B18	23.0	.65	MX8	5.0	.22
B19	3.0	.94	MX9	16.0	.22
B20	23.0	.60	MX10	4.0	.22
M1	5.0	.36	MX11	10.0	.22
M2	15.0	.36	MX12	29.0	.22
M3	25.0	.36	C1	0.0	approx 1x1x.25 cm
M4	30.0	.36	C2	10.0	1x1x.25
M5	5.0	.41	C3	5.0	1x1x.25
M6	15.0	.41	C4	20.0	1x1x.25
M7	0.0	.23	C5	15.0	1x1x.25
M8	0.0	.29	C6	30.0	1x1x.25
M9	0.0	.41	C7	25.0	1x1x.25
M10	0.0	.36	C8	40.0	1x1x.25
M11	10.0	.23	C9	50.0	1x1x.25

where:

A = Indian River Inlet, Delaware
B = Delaware Bay, Delaware
M = Michigan Coastline (Sleeping Bear State Park, Petosky State Park, Mason-Oceana County Line, Pentwater State Park, and Muskegon State Park)
H = South Beach and Glen Eden Beach, Oregon Coastline
MX = Panama City, Florida (Gulf of Mexico)
C = Marine Carbonate, Florida Keys

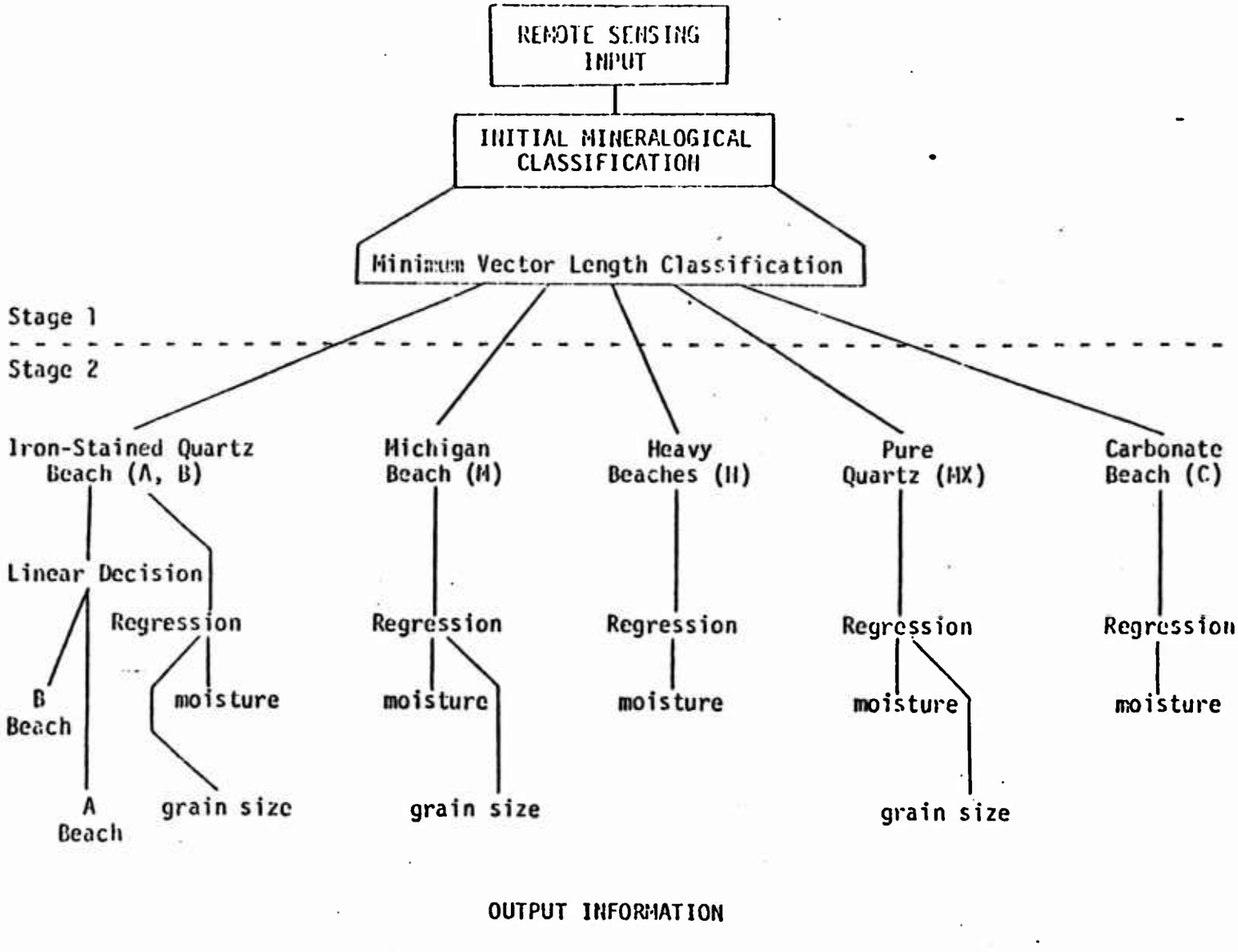

FIGURE 1. FLOW DIAGRAM OF THE MOGS ALGORITHM.

a breakdown of sand mineralogy into discrete classes. Within each class, second stage multiple linear regressions were used to derive the moisture and grain size information. Using this method the second stage regressions do not have to account for the large spectral effects of mineralogy characteristic of diverse beach sands. This division increased the accuracy and predictive ability of the moisture and grain size regression equations considerably.

In order to determine which spectral regions would best be able to differentiate and predict the parameters of interest, the AQUASAND beach sand model was used. By varying the model input parameters in a logical fashion it was possible to predict what regions of the spectrum yielded the most useful information. These spectral regions were then used in the MOGS algorithm to predict the parameters of interest. Because the MOGS algorithm is to be used on aircraft collected multispectral scanner (MSS) data, all the input spectral data were divided into 17 spectral "bands" which are feasible (dictated by atmospheric transmittance) for implementation using existing MSS technology (Table 2). In any given portion of the MOGS algorithm only a subset of these 17 bands were used, as will be shown later.

The Prediction of Mineralogy

Rather than attempting to predict the individual mineral components of the different sands it was decided that grouping the sands into homogeneous types would be more productive. As such, five groups were defined which, for the most part, corresponded with the geographic location of collection of the data base samples. The five mineralogical classes are as follows:

1. Iron-stained Atlantic coast type (A, B),
2. Iron-stained Michigan type (M),
3. Non-Iron-stained pure quartz type (MX),

TABLE 2

The 17 spectral bands used in the development of moisture and grain size regression equations

Band #	Wavelength Range (um)
1	0.43-0.47
2	0.47-0.49
3	0.49-0.51
4	0.51-0.53
5	0.53-0.56
6	0.56-0.59
7	0.59-0.63
8	0.63-0.67
9	0.70-0.75
10	0.75-0.80
11	0.80-0.90
12	0.90-1.00
13	1.00-1.10
14	1.10-1.20
15	1.20-1.35
16	1.50-1.85
17	2.10-2.50

TABLE 3

The eight spectral bands used in the breakdown of beach mineralogy into one of five categories. In addition to these eight bands all unique ratio combinations were also used.

Band #	Wavelength Range (um)
1	.43-.47
2	.47-.49
3	.51-.53
4	.53-.56
5	.59-.63
6	.80-.90
7	.90-1.0
8	1.0-1.1

4. Heavy mineral (dark sand) type (H),

5. Carbonate type (C).

Typical spectra of these five mineralogical categories is given in Shuchman, et al, (1978). To discriminate the five mineralogical classes a minimum-vector-length decision framework was used. The concept is developed as follows. Suppose that there are two points, A and B, located in two-dimensional space. The distance, or vector length, L, from A to B can be expressed in terms of the X and Y locations of points A and B as

$$L = \left[(X_A - X_B)^2 + (Y_A - Y_B)^2\right]^{\frac{1}{2}} \quad . \tag{1}$$

This is, of course, related to the Pythagorean Theorem. Now suppose we have a p-dimensional system with A and B located in each dimension. The vector length can be expressed as

$$L = \left[\sum_{i=1}^{p} (X_{iA} - X_{iB})^2\right]^{\frac{1}{2}} \quad , \tag{2}$$

where X_{iA} is the location of point A in the ith dimension and X_{iB} is the location of point B in the ith dimension.

This rationale can be used to classify some point, T, as being the member of one of n classes (A_j, j = 1,n), by finding the minimum vector length from T to A_j (j=1,n). In other words T is said to be a member of the class which is closest to it, on the average, across all p dimensions. The minimum vector length is defined as

$$L_{min} = \min_{j=1,\ldots,n} \left[\sum_{i=1}^{p} (X_{iT} - X_{iAj})^2\right]^{\frac{1}{2}} \quad . \tag{3}$$

Notice that equation 3 has no provision for variability in the n classes, therefore, L_{min} is chosen as being the shortest linear vector length. If each class has the same variability associated with it this causes no difficulty. In this experiment, however, there were considerable differences in variability between the classes so that a modification of equation 3 had to be made. The standard deviation (SD) was used to modify the distance between T and A_j related to each dimension thus removing the effects of variability from each class. This normalized minimum distance equation is expressed as

$$L_{min} = \min_{j=1,\ldots,n} \left[\sum_{i=1}^{p} \left[(X_{IT} - X_{iAj})/SD_{ij} \right]^2 \right]^{\frac{1}{2}} , \qquad (4)$$

where SD_{ij} is the standard deviation associated with the jth class in the ith dimension.

In the application of this method to the classification of mineralogy, the "dimensions" are spectral bands or ratios of spectral bands and the "classes" are mineralogical types. Eight spectral bands (Table 3) and all possible unique ratios of those spectral bands were used to classify the mineralogical type of an input sand as one of five categories. The object was to make each category as homogeneous as possible so that the moisture and grain size regressions which followed would be sensitive to small scale spectral changes.

The Prediction of Moisture and Grain Size

Using the AQUASAND model we found that information related to moisture content of sands is best derived from the spectral region beyond 1.0 μm. This is the result of the spectral reflectance of sand in this region being

reduced by absorption in proportion to the amount of water present. (Exceptionally high spectral absorption is noted near 1.4 and 1.9 μm.) Although the spectral reflectance in these regions is highly correlated to moisture we did not consider them since atmospheric absorption prohibits their use by an airborne sensor.

Changes in grain size seem to manifest themselves most clearly in the shorter wavelengths (0.4-0.7 μm). Grain size information is gained by light being reflected from sand grains below the surface through surface grains. The transmittance through the surface grains is reduced by internal scattering and absorption of the particle. Since both of these factors are dependent on thickness, the bulk reflectance of a sand is dependent to some degree on the grain size. Theoretically a coarsely grained sand should have a lower reflectance than a fine grained sand of the same mineralogical composition, surface frosting, and with similar moisture content. According to our measurements this appears to be the case.

This grain size phenomenon can be confounded in two ways. First, if there is no scattering or absorption within the grains (i.e., a perfectly clear material at all wavelengths) there can be no attenuation. Fortunately, even in our purest quartz sands there were enough impurities and inclusions to give some attenuation. Second, the sand grains may be opaque and thus attenuate too much light. This appears to be the case in the heavy mineral and carbonate beaches. Most of the bulk reflectance for these two types was the result of surface reflectance and essentially none from light transmitted through the surface grains from below. We were unable to create accurate grain size equations for these types.

Utilizing the physical phenomena discussed above we were able to develop multiple linear regression equations for predicting moisture in all five mineralogical classes and grain size for three of the five mineralogical classes. The basis for all the regressions, except one, was the sample group corresponding to a given mineralogical class. The single exception was the grain size equation corresponding to a pure quartz beach. Our samples within this type consisted of a single grain size (0.22 mm) and, as such did not provide an adequate basis for regression equations. For this case we used AQUASAND generated spectra to simulate a wide range of grain sizes in order to add grain size variability to the data set.

Seventeen spectral bands between 0.4 and 2.5 μm were chosen for use in the regressions (Table 2). Within the 17 bands, only those which were predicted by the AQUASAND model to be most informative were used. In this way we could be reasonably certain that the regression equations would respond the correct parameter and thus yield accurate predictions. The predictive equations together with the associated standard errors (SE), and coefficient of variation (R^2) are given in Table 4.

In summary, the MOGS algorithm represents (see Figure 1) a computer controlled package of equations. The input is a set of 17 spectral reflectance bands obtained from an unknown sand. Based on these bands, the sand is classified as being a member one of five mineralogical types. Depending on the mineralogical type, the appropriate moisture and grain size (where applicable) equations are applied to the data. The output from the MOGS algorithm is the predicted mineralogical class, the predicted moisture, and the predicted grain size.

TABLE 4

Multiple linear regression equations for the prediction of moisture and grain size. The equations are listed by mineralogical class. Grain size is in mm.

a. Iron stained quartz* - Atlantic coast

Predicted moisture % = $67.964 - 65.046 \left(\frac{\text{Band 16}}{\text{Band 14}}\right)$

S.E. = $\pm$ 3.08%, $R^2 = 0.888$

Predicted grain size = $6.87 - 3.4634 (\text{Band 7})^{1/4} + .0300 (\text{Band 1}) + .01672(\text{Band 15})$

S.E. = $\pm$ 0.13 mm, $R^2 = 0.603$

b. Iron stained quartz - Michigan coast

Predicted moisture % = $60.149-49.961 \left(\frac{\text{Band 16}}{\text{Band 11}}\right)-2.226 \left(\frac{\text{Band 17}}{\text{Band 1}}\right)$

S.E. = $\pm$ 2.56%, $R^2 = 0.970$

Predicted grain size = $0.6405-0.0152 (\text{Band 5}) - .0047 (\text{Band 17})$

S.E. = $\pm$ 0.055 mm, $R^2 = 0.558$

c. Non-Iron stained quartz

Predicted Moisture % = $127.02-65.159 \left(\frac{\text{Band 16}}{\text{Band 15}}\right) - 64.054 \left(\frac{\text{Band 15}}{\text{Band 14}}\right)$

S.E. = $\pm$ 2.12%, $R^2 = 0.971$

Predicted grain size = $1.158-2.328 (\text{Band 10}) + .3201 \left(\frac{\text{Band 7}}{\text{Band 1}}\right) + 0.2858 (\text{Band 10}$

S.E. and R^2 not applicable

d. Carbonate

Predicted moisture % = $596.28-642 \left(\frac{\text{Band 14}}{\text{Band 17}}\right) - 1.081 (\text{Band 14}) + 0.1538 (\text{Band 17})$

S.E. = $\pm$ 4.09%, $R^2 = 0.879$ No grain size equation.

e. Heavy mineral

Predicted moisture % = $19.284 + 11.194 \left(\frac{\text{Band 14}}{\text{Band 17}}\right) - 1.081 (\text{Band 14}) + 0.1538 (\text{Band 17})$

S.E. = $\pm$ 4.09%, $R^2 = 0.879$ No grain size equation

* Iron stain quartz was determined by visual examination under stereo-microscope.

TEST RESULTS OF THE MOGS ON LABORATORY SPECTRA

The MOGS algorithm was first tested on 70 of the 81 samples from which it was derived and the results were very promising. Eleven samples were discarded because their grain sizes were abnormally large or percent moisture was inaccurate. The classification of mineralogy was 99+% correct. The overall correlation of predicted to actual moisture was 96% (significant at the 0.001 level) and the overall correlation of predicted to actual grain size was 88% (significant at the 0.001 level). However, testing any equation or algorithm on the samples from which it was derived is not conclusive. For this reason the MOGS algorithm was tested on several other beach sand samples which were independently collected and spectrally measured following the algorithm construction. These results are given in Table 5. In each case the MOGS algorithm selected a mineralogy which allowed the moisture and grain size regression to operate correctly. The independent test yielded an actual moisture to predicted moisture correlation of 0.95 (significant at the 0.01 level). The prediction of grain size was in no case more than 0.07 mm different from the actual grain size.

TEST OF THE MOGS ALGORITHM ON MSS DATA

The next logical test for the MOGS algorithm was to evaluate it on actual multispectral scanner (MSS) data. Such an investigation was carried out using aircraft data obtained from the ERIM-MSS. The ERIM-MSS (Hasell, et al, 1974) is an optical scanning device, i.e., it receives signals continuously while the sensor instantaneous field of view (IFOV) moves over the flight path scanning the terrain. The MSS is a passive device, meaning it senses energy originating from the sun and reflected from the terrain. The data from the MSS used in this analysis covered 12 discrete spectral

TABLE 5

Comparisons of actual parameters to predicted classifications by the MOGS algorithm. Samples used here were collected independently of those on which the algorithm is based.

Sample Mineralogy		Moisture %			Mean Grain Size (mm)		
Actual	Predicted	Actual	Predicted	Percent Different	Actual	Predicted	mm Different
MICH1	MICH	37.7	25.6	-12.1	.26	.28	+ .02
MICH2	MICH	3.2	3.7	+ .5	.28	.30	+ .02
MICH3	MICH	0.3	0.0	- .3	.25	.32	+ .07
MICH4	MICH	12.1	16.0	+ 3.9	.23	.29	+ .06
MICH5	MICH	15.0	12.7	- 2.3	.25	.30	+ .05
MICH6	MICH	28.0	26.2	- 1.8	.28	.29	+ .01

TABLE 6

Spectral bands used by ERIM-MSS for testing the MOGS algorithm

Band Number	Range (μm)
1	0.40-0.44
2	0.43-0.46
3	0.45-0.49
4	0.48-0.53
5	0.51-0.57
6	0.54-0.63
7	0.60-0.72
8	0.66-0.84
9	0.78-1.1
10	1.2 -1.4
11	1.5 -1.8
12	2.0 -2.6

bands in the 0.4 to 2.5 μm region of the electromagnetic spectrum (see Table 6).

Field Test

Multi-Spectral Scanner data were collected over three test sites along the Michigan shoreline; Muskegon State Park, Pentwater State Park, and Mason-Oceana (M-O) County line. The flight, part of an ERIM flight test for a NASA and NOAA program, took place on 1 November 1978 under clear skies between 1:00 and 2:00 P.M.

Coincident with the fly-over, the following ground truth survey was carried out at the Pentwater test site:

1. sand samples were collected to confirm grain size and moisture conditions at the time of flight, and
2. reflectance panels (black and gray) were placed on the beach and radiance and irradiance spectral measurements obtained.

Additionally, three sand samples were taken at the M-O County line site and two sand samples obtained along with a reflectance measurement at the Muskegon State Park test site.

The Michigan beach test was the first test of the MOGS algorithm on actual MSS data. The bands available on the ERIM-MSS (M7) as it presently functions necessitated a change in the band classification using the MOGS algorithm. The algorithm was changed to handle a total of 12 instead of 17 bands. This was simply done by truncating the five bands from the algorithm not available on the ERIM-MSS(M7). The resulting predictions of mineralogy using 12 instead of 17 were not affected. Using only five bands and ten ratios, the algorithm classified the mineralogies very well. This indicates that the use of eight bands and 26 ratios, as in

the original algorithm, is probably over precision. In addition, the M7 bands give very nearly the same predictions for moisture and grain size for the Michigan beaches as the 17 bands which were used to develop the original equations.

Aircraft MSS Data Reduction

Table 6 lists the 12 channels of MSS data used in the Michigan tests. These channels (as mentioned previously) were selected as being very close to the channels used in the development of the MOGS algorithm. The nine channels corresponding to the shorter wavelengths utilized a photo-multiplier detection system while the three longer wavelength channels used an InSb (lead sulfide) detector. The data were recorded digitally on a High Density Digital Tape (HDDT) for later computer processing.

Using an ERIM computer video display, the exact location of the test sites were determined and the data for all three test sites were transferred to a computer compatible tape (CCT) for use on the University of Michigan AMDAHL 470 computer system (MTS). Rather than converting all the data, only an area 100 pixels on either side of the test site was recorded for each test site. Each pixel for the test data (600 meter altitude) is approximately a 1.5 meter square. The use of only 100 pixels on either side of the test site negated having to correct the aircraft data for scanning angle effects of the sensor.

Using the generated CCT on MTS, gray maps (computer generated images) were produced to ascertain the exact areas from which the sand samples were collected. Upon specific location of the sample areas within the test site, the actual digital values obtained by the remote sensor were extracted. The data values obtained from MTS corresponding to the sample areas were then

tabulated and "calibrated". This was accomplished by using an MTS module to extract the calibration values related to each scan line which contained a sample point. The "black body" calibration value was subtracted from the sample value for each sample to normalize the data. We found essentially no variability between scan lines in terms of the calibration values.

Concurrent with the data extraction, the sand samples obtained from the test site were measured for reflectance using the Cary 14 spectrophotometer. The signal values obtained from the scanner data were then plotted against the appropriate band reflectance, as measured with the Cary 14, to achieve a signal value to reflectance transfer curve. For some reason, probably related to the non-Lambertian nature of objects in the scene, the relationship did not appear to be strictly linear in all bands. This non-linearity appears to be most pronounced for the near infrared spectral bands which use the InSb detector. In addition, the reflectance calibration panels which were deployed at the Pentwater Site do not plot well with the sand values. This means that, in this case, the panels were not particularly useful in calibrating the MSS system to values of reflectance. Our final signal-value-to-surface reflectance calibration was accomplished using the reflectance of a few sand samples (four) plotted against the MSS digital signal value. The digital values of other areas on the beach were then altered to reflectance using these curves. Thus the ERIM-MSS(M7) received radiance value was converted to a reflectance value using this technique.

Aircraft Test Results

The test results using the aircraft scanner data are encouraging (Table 7). The correlation (R) of predicted to actual moisture content is 0.91 (significant at the 0.01 level) and the prediction of grain size is, in no case, greater than 0.09 mm different from the actual grain size. The

TABLE 7

Comparison of actual parameters to predicted classifications by the MOGS algorithm. The sand spectra used here were collected by the ERIM-MSS

Sample Mineralogy		Moisture %			Grain Size (mm)		
Actual	Predicted	Actual	Predicted	Percent Different	Actual	Predicted	mm Different
Pentwater	MICH	22.3	12.1	-10.2	.25	.32	+ .07
Pentwater	MICH	1.0	0.0	- 1.0	.23	.28	+ .05
Pentwater	MICH	8.0	10.1	+ 1.9	.22	.25	+ .03
Pentwater	MICH	28.0	16.9	-11.1	.26	.35	+ .09
Pentwater	MICH	5.0	2.2	- 2.3	.24	.26	+ .02
M-0 Line	MICH	Not Measured			.29	.32	+ .06
M-0 Line	MICH	Not Measured			.27	.36	+ .09
M-0 Line	MICH	Not Measured			.29	.37	+ .08
Muskegon St. Pk.	MICH	Not Measured			.25	.30	+ .05

predicted grain sizes shown in Table 7 are all larger than the actual measured grain size. The statistical analysis on the sand samples used to create the Michigan grain size regression equation showed the sands to be moderate to well sorted (i.e., low standard deviation of grain size) but exhibiting a negative skewness in almost all cases. This negative skewness, indicative of a coarse fraction, could have biased the grain size prediction algorithm and caused the larger than actual prediction of grain size to result.

The moisture prediction appears particularly poor for high moisture contents. This is most likely the result of wet sand at the test sites exhibiting bi-directional dependencies (i.e., a failure to behave in a Lambertian manner). These bi-directional characteristics are enhanced at low sun angles and are not accounted for by the MOGS algorithm. Although the flight took place at 1:30 EST the sun was only 38° above the horizon on November 1.

A laboratory experiment was conducted to quantify the effects of bi-directional dependencies of wet sand. Figure 2 shows the laboratory set-up used to conduct the test. The sand was spread evenly in a 70 x 70 cm tray to a depth of 2.5 cm. Illumination was provided by a 200 µw projector lamp whose beam was optically collimated to provide a highly directional source(i.e.≈6°) The detector used was a Coherent Optics power meter which utilized a silicon detector. The aperture of the detector was reduced using baffles such that an area approximately 5 cm square on the sand surface was sensed. To avoid having the detector head shadowing the sand it was offset such that it was viewing at an angle of 23° from the vertical. As is shown in Figure 2, the lamp was moved through several angles from normal to the sand surface to nearly parallel with it. At each angle the flux to the detector was measured and recorded.

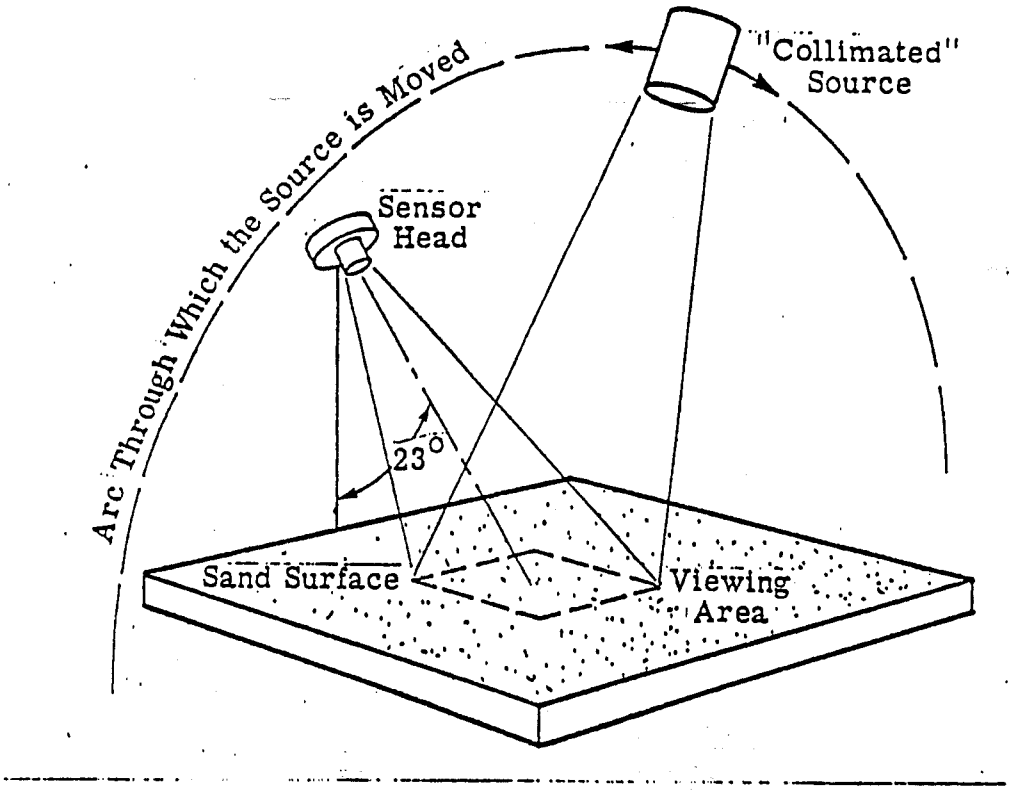

FIGURE 2. EXPERIMENT SET-UP USED TO DETERMINE LAMBERTIAN PROPERTIES OF SAND.

According to theory, if a surface is perfectly Lambertian then the exitance from the surface should decrease with the cosine of the angle of incidence. Therefore the exitance observed at any illumination angle should be equal to the exitance with the illumination normal to the surface multiplied by the cosine of the angle of interest. Using this relationship, a useful measure of the Lambertian nature of a material is

$$R = \frac{M_\theta}{M_0 \cos \theta} \quad , \tag{5}$$

where R is the measure of Lambertian nature, M_θ is the exitance observed at illumination angle θ and M_0 is the exitance observed with the illumination normal to the surface. For a perfectly Lambertian material R should be 1.0 for all θ. If R is less than 1.0 then less flux is being reflected at angle θ than was expected, and if R is greater than 1.0 the reverse is true.

Using the experimental design just described, two sand conditions were investigated: dry sand and sand with ~25% moisture. As can be seen in Figure 3A, dry sand is quite Lambertian in character at angles up to 60° incident (30° above the horizon). The sun angle during the Michigan test flight was approximately 52° incident indicating the exitance from dry sand was ~84% of that expected from a Lambertian material. This is in fact quite good for this incidence angle although a more nearly normal incidence angle (higher sun) would have been desirable.

The wet sand (Figure 3B) exhibits strong bi-directional properties indicative of a semi-specular surface. The raw data indicates a very high

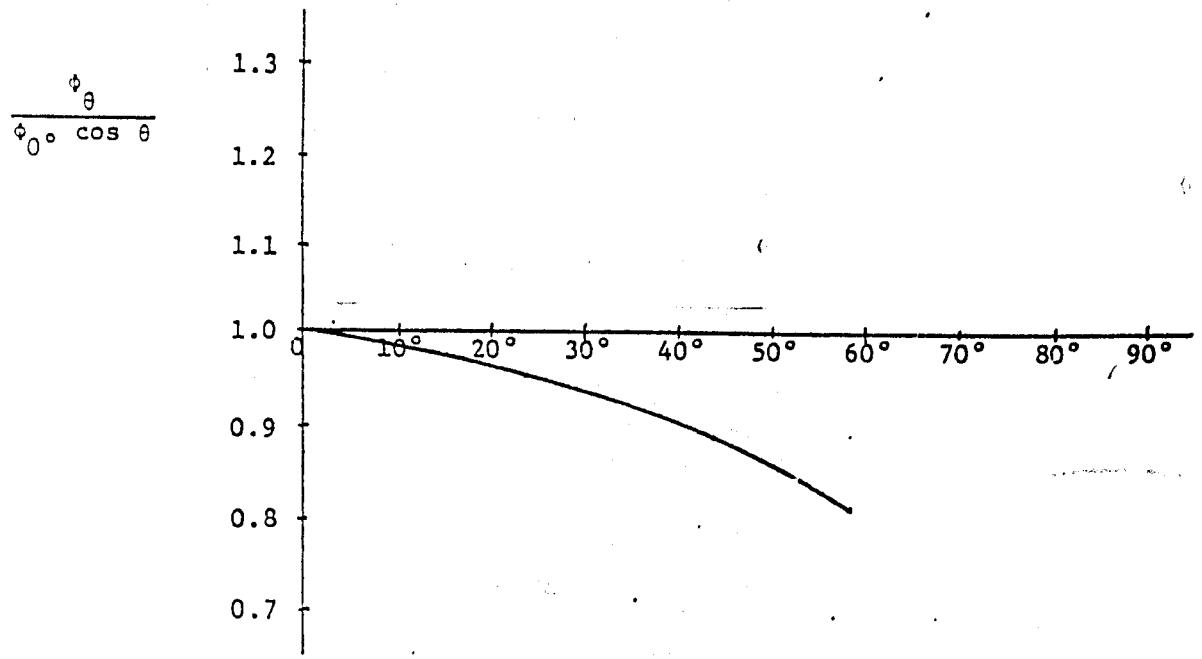

FIGURE 3A. DRY SAND CASE

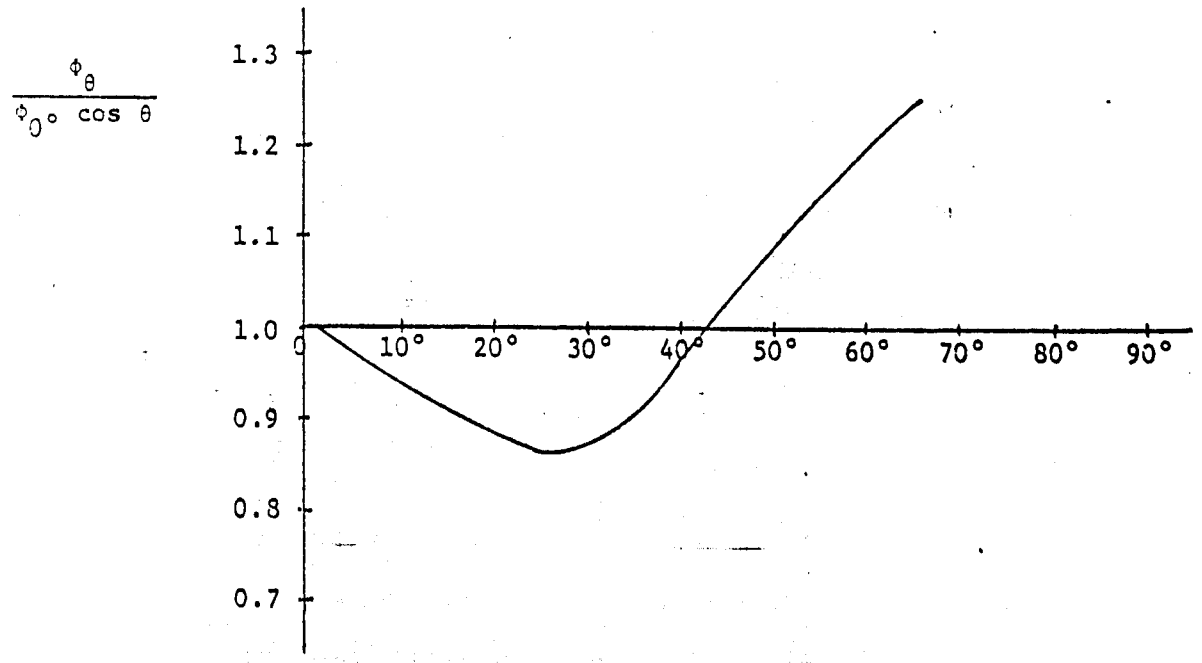

FIGURE 3B. WET SAND CASE

exitance at 0° incidence followed by a rapid fall off at other incidence angles relative to that observed for dry sand. The implication is that there is a specular return at 0° incident--a very non-Lambertian characteristic; for such a case the assumption of a Lambertian surface does not hold. Note from Figure 3 that for sun angle ±15° from zenith that wet and dry sands decrease in reflectance approximately the same amount and therefore minimize non-Lambertian effects. It should be noted that the goniometric study described was not a spectral study but rather used a light source that ranges the visible and is weighted to the infrared.

In summary, the Cary 14 Spectrophotometer makes a reflectance measurement that is hemispherical, i.e., the reflectance properties whether bi-directional, Lambertian, or diffuse have little bearing on the reflectance that is sensed. Conversely, the MSS only intercepts radiation which is reflected in a certain direction as opposed to the diffuse sensing of a spectrophotometer. For an MSS, this sensing is normal to the sensed surface at the center of the scan and progressively more oblique toward the edges of the scan. The type of illumination is highly variable ranging from diffuse with an overcast sky to nearly specular on a clear sunny day. In the former case, the geometry is much like that of a spectrophotometer in reverse--diffuse source and specular sensing. Because of reciprocity the apparent reflectance as derived from MSS data ignoring path radiance factors should be exactly the same as the reflectance sensed by a spectrophotometer. Thus, to minimize bi-directional reflectance, future aircraft flights should be made during complete mid-altitude (3000 m) cloud cover or sunny skies with the sun close to the zenith (summer sun) as indicated from Figure 3.

Applying the same moisture and grain size equations used in the previous analysis, the entire Pentwater State Park beach on a pixel-by-pixel basis (in this case 1.5 x 1.5 meters) was classified with respect to grain size and

moisture content. The two MOGS generated digital maps (see Figure 4) show the predicted moisture and grain size distribution on the beach at Pentwater. Also included on Figure 4 is a panchromatic aerial photograph take coincident with the MSS data. The ground truth measurements taken at the time of flight correlate well with these images. Figure 4 helps to demonstrate how potentially an entire sandy coastline could be analyzed in respect to moisture, grain size, and gross mineralogy using a small subsection as calibration.

CONCLUSION

The development of the MOGS algorithm has demonstrated the feasibility of obtaining quantitative moisture and grain size information from the spectral reflectance of beach sands. The determination of grain size is dependent on the sand grains being neither opaque nor perfectly clear.

The two stage nature of the MOGS algorithm is directly responsible for its broad applicability without loss of detail. By separating the mineralogical types prior to the prediction of moisture and grain size much of the variability which could easily hide small scale changes is removed. The use of a vector-length discriminant function to classify mineralogy worked extremely well in this application, since 36 different dimensions could be evaluated simultaneously. A multistage approach involving multiple classification techniques is a powerful tool, one which may be very useful in many areas of remote sensing.

The Lake Michigan field test has further demonstrated the MOGS algorithm's applicability to remotely sensed field data. Grain size was predicted to

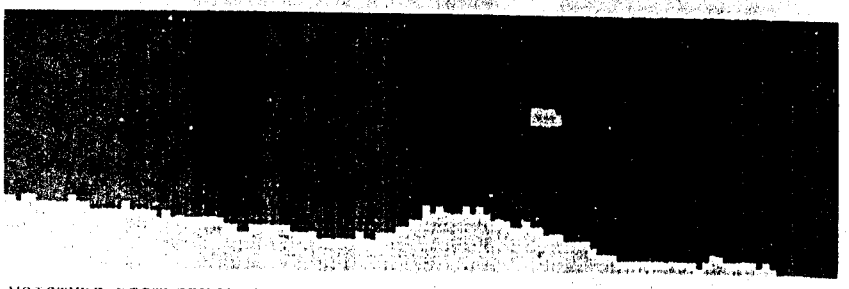

MOISTURE DISTRIBUTION IMAGE - LIGHTER SHADE INDICATES HIGHER MOISTURE CONTENT

0-5% 5-20% 20+%

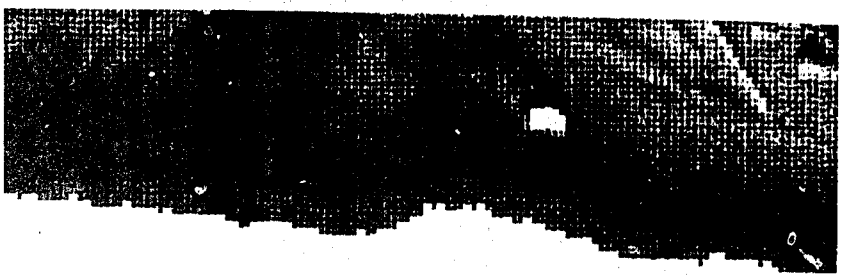

GRAIN SIZE DISTRIBUTION IMAGE - LIGHTER SHADE INDICATES LARGER GRAIN SIZE

.15-.25 mm .25-.40 mm >.40 mm

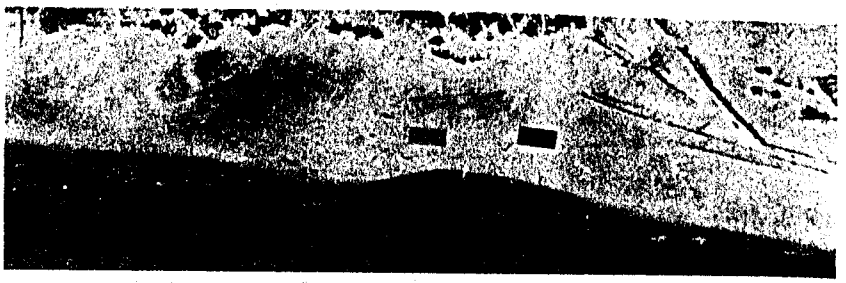

PANCHROMATIC AERIAL PHOTOGRAPH

FIGURE 4. DIGITAL IMAGERY, GENERATED BY THE MOGS ALGORITHM SHOWING THE DISTRIBUTION OF MOISTURE AND GRAIN SIZE ON PENTWATER BEACH (PENTWATER STATE PARK, MICHIGAN). WHITE AREAS ARE EITHER UNCLASSIFIED REGIONS OR OPEN WATER.

within 0.09 mm mean diameter of the actual size while beach moistures below 20% were accurately predicted. In all cases the computer algorithm correctly identified the Michigan beach mineralogy as being a predominately iron-stained, quartz-feldspar beach.

ACKNOWLEDGEMENTS

This work was supported by the Office of Naval Research (ONR) contracts N0014-74-C-0273 and N0014-78-C-0458. Mr. Hans Dolezalek of ONR served as the technical monitor on both contracts. The Rackham Graduate School, The University of Michigan supported the collection of beach sands along Lake Michigan and the ensuing laboratory analysis of the sand parameters. Ms. Karla Amble of the Environmental Research Institute of Michigan (ERIM) performed the majority of the laboratory analysis of the sand parameters.

Mr. Carl Davis, formerly of ERIM, now with Eaton Stamping Company, is acknowledged for creating, as well as operating, the computer software necessary to perform this research.

The authors would like to thank Dr. Gwynn Suits, Mr. Fred Thomson, and Dr. Philip Jackson of ERIM for their guidance and critical review of the work presented in this paper. Ms. Kathleen Newstead of ERIM is thanked for her typing of the manuscript.

REFERENCES

Aronson, J. R., et al. (1967), Studies of the middle- and far-infrared spectra of mineral surfaces for application in remote compositional mapping of the moon and planets, Journal of Geophysical Research, 72, (2), 687-703.

Emslie, A. G. (1966), Theory of diffuse spectral reflectance of a thick layer of absorbing and scattering particles, in thermophysics and temperature control of spacecraft and entry vehicles, Progress in Astronautics and Aeronautics, 18, (G. B. Heller, Ed.), Academic Press, New York.

Fraser, G. S. and N. C. Hester (1977), Sediments and sedimentary structures of a beach-ridge complex, southwestern shore of Lake Michigan, J. Sed. Petrol., 47, p. 1187-1200.

Hasell, P. G., et al (1974), Michigan experimental multispectral mapping system: a description of the M7 airborne sensor and its performance, Technical Report 190900-10-T, Environmental Research Institute of Michigan, Ann Arbor.

Hunt, G. R. and R. K. Vincent (1968), The behavior of spectral features in the infrared emission from particulate surfaces of various grain sizes, Journal of Geophysical Research, 73 (18), 6039-6046.

Huntley, D. A. and A. J. Bowen (1975), Comparison of the hydrodynamics of steep and shallow beaches, in: J. Hails and A. Carr, eds., Nearshore Sediment Dynamics and Sedimentation, John Wiley & Sons, New York, 69-109.

Komar, P. D. (1976), Beach processes and sedimentation, Prentice-Hall, Inc., Englewood Cliffs, N.J., 429 p.

Komar, P. D. (1977), Selective longshore transport rates of different grain-size fractions within a beach, J. Sed. Petrol., 47, 1444-1453.

Leu, David J. (1977), Visible and near-infrared reflectance of beach sands: a study on the spectral reflectance/grain size relationship, Remote Sensing of Environment, Vol. 6, No. 3, 169-182.

Madsen, O. S. and W. D. Grant (1976), Quantitative description of sediment transport by waves in: Proc. 15th Coastal Eng. Conf., Am. Soc. Civil Eng., New York, 1093-1112.

Self, R. P. (1977), Longshore variation in beach sands, Nautla area, Veracrus, Mexico, J. Sed. Petrol., 47, 1437-1443.

Shuchman, R. A., G. H. Suits and C. F. Davis (1978), AQUASAND: a beach reflectance model and validation tests, Proceedings of Fifth Canadian Symposium on Remote Sensing of Environment, Victoria, British Columbia, Canada.

Suits, G. H. (1972), The calculation of the directional reflectance of a vegetation canopy. Rem. Sens. of Env., Vol. 2, 117-125.

Swart, D. H. (1976), Predictive equations regarding coastal transports, in: Proc. 15th Coastal Eng. Conf., Am. Soc. Civil Eng., New York, 1113-1132.

Vincent, R. K., F. J. Thomson and K. Watson (1972), Recognition of exposed quartz sand and sandstone by two-channel infrared imagery. J. Geophys. Res., 77, 2473-2477.

Zenkovich, V. P. (1967), Processes of coastal development, Interscience, New York, 738 p.

END